# THE EFFECT OF CURVATURE ON THE TRANSITION FROM LAMINAR TO THE TURBULENT BOUNDARY LAYER

Thesis by

Milton Clauser
and
Francis Clauser

In Partial Fulfillment of the Requirements for the Degree of Doctor of Philosophy

California Institute of Technology

Pasadena, California

1937

TABLE OF CONTENTS

INDEX TO FIGURES

INDEX TO PHOTOS

1. Fan Assembly Detached from Diffuser.
2. Fan about to be Mounted.
3. Fan Assembly and Diffuser.
4. Diffuser Section.
5. Straight Working Section.
6. Curved Working Section.
7. Framework of Curved Working Section.
8. Micrometer Carriage Hot-Wire Holder.
9. Exit Diffuser.
10. Hot-Wire Amplifier.
11. Calibrating Tunnel.

## NOTATION

$x$=Distance along sheet from leading edge.

$y$=Distance normal to the sheet.

$r$=Radius of curvature of sheet.

$u$=Local velocity in x direction.

$U$=Mean free-stream velocity.

$v$=Local velocity in y direction.

$R_x$=Reynolds Number based on length x and velocity U.

$R_y$=Reynolds Number based on length y and velocity U.

$\delta$=Boundary layer thickness.

$p$=Local pressure.

$u' = \sqrt{\overline{u^2}}$

$\Delta_o$=Double amplitude of vibration of wire in calibrating tunnel.

$\omega$=Frequency of same.

$P_s$=Static pressure in calibrating tunnel.

$k$=Calibration constant of $P_s$ against $\frac{1}{2}\rho U^2$ in calibrating tunnel.

$\gamma$=Density of alcohol in manometer.

$\rho$=Density of air.

$\nu$=Kinematic viscosity of air.

ACKNOWLEDGMENT

The authors' wish to thank Drs. Karman and Millikan for their constant interest and guidance in the experimental program; Drs. Klein and Sechler for their many helpful suggestions on the design of apparatus; and Mr. A. C. Charters for his help and cooperation while working on his part of the project.

Further, the authors' wish to thank their sister, Miss Celeste Clauser for her part in typing and preparing the manuscript.

SUMMARY

In the flow over the upper surface of a wing, a discrepancy between the predicted and actual point of transition from laminar to turbulent boundary layer had been found. This effect may be due to the comparatively small radius of curvature of the upper surface of the wing. The present tests were undertaken to investigate this effect.

As no available channel was suitable for this work, a new channel with two working sections was built. One working section had a wall with a twenty inch radius of curvature and the other section had a flat wall.

Three types of measurements were made: a. Traverses were made with a total head tube to determine the character of the boundary layer at various Reynolds Numbers. b. The turbulence distribution in the boundary layer was investigated by means of a hot wire and vacuum tube amplifier. c. A similiar investigation of the mean velocity distribution in the boundary layer was made by means of a hot wire anemometer.

It was found that by using an abreviated form of the turbulence level traverses, critical Reynolds Numbers for the transitions could be established. These critical Reynolds Numbers are plotted as a function of $\frac{x}{r}$ (x being the distance of the transition from the leading edge of the plate; r being radius of curvature of the plate) for both the convex and concave side of the plate.

INTRODUCTION

In practically every article on the performance of the modern high speed airplane, can be found a statement to the effect that since great strides have been made in "cleaning up" airplanes aerodynamically, the points which once seemed unimportant have recently become the focus of the designer's attention. This is particularly true of the skin friction drag.

It has long been known that for a certain range of Reynolds Numbers the laminar skin friction coefficient is much smaller than the turbulent skin friction coefficient for any Reynolds Numbers obtainable in practice. It has also been discovered that the transition from laminar to turbulent boundary layer on the top surface of a wing occurs at a point much farther back on the wing than would be predicted from transition measurements made on a flat plate. The primary cause of this discrepancy was thought to be due to the effect of the very high curvature of the upper surface of the wing on the boundary layer. It was to investigate this point that the present series of tests were inaugurated.

DESIGN OF APPARATUS AND EQUIPMENT

When this series of tests was started the only channel which was at all suited for this work was a small one which had previously been used by Wattendorf* in determining the effect of curvature on fully developed turbulent flow. This channel had several disadvantages. It operated at subatmospheric pressure which caused the walls to deflect inward as the speed increased. At the same time, any hole admitting measuring instruments might also admit enough air to seriously disturb the flow. The channel was so small that difficulty had been experienced in using correspondingly small measuring instruments. The last but perhaps the most important disadvantage was that the channel was not easily adaptable to starting the boundary layer with zero thickness at the beginning of the curvature.

With this in mind, it was decided to build a new channel which would overcome these difficulties. To prevent wall deflections the new tunnel would have to operate at atmospheric pressure. This was accomplished by putting the fan**

*Wattendorf, F. L., A Study of the Effect of Curvature on Fully Developed Flow. Proc. of Roy. Soc. of London, Series A, Vol. 148 pp.565-598. Feb. 1935.

**For a detailed description of the component parts of the channel, see Appendix I.

ahead of the working section (see Fig.1). In this arrangement the pressure drop across the fan is approximately equal to the dynamic pressure in the working section (except for friction losses and the expansion at the exit.) In order to damp out the turbulence of the fan, a large pressure box (see Fig. 1) which had been used on another tunnel was added between the fan and the working section. In this box were placed two screens comprised of several layers of cheese cloth which served to damp out the large eddies and gave a uniform flow of very fine scale turbulence which damped out before the air reached the working section. Behind the fan was also placed a diffuser by means of which some of the kinetic energy of the air ($\frac{1}{2}\rho V^2$) was converted into pressure before it entered the box. To prevent undesirable drafts and eddy curents in the room, another diffuser was placed after the working section. Into this diffuser were built two screens to create a pressure drop to counteract the pressure rise of the diffusion.

A great deal of thought was given to the design of the working section (for details see Appendix I). It was desirable to have the channel as large as possible and yet have a favorable aspect ratio to assure two dimensional flow. The channel was made as tall as the pressure box which was seven feet high. A twelve to one aspect ratio was decided upon which made the channel seven inches wide. In order that the boundary layer start with zero thickness, measurements were made on a sheet suspended midway between the side walls and extending the full height of the channel. This presented both a convex and concave

surface of the same radius of curvature. As only the effect of curvature was desired, any pressure gradient in the channel was eliminated by making the side walls adjustable.

The choice of the radius of curvature was more difficult. The teoretical aspects of the problem were first investigated. The amount of curvature may be expressed numerically by the parameter $\frac{\delta}{r}$ where $\delta$ is the boundary layer thickness and r is the radius of curvature of the wall. Since the boundary layer thickness is a function of the distance x which the flow has traveled along the plate, we may replace this parameter by $\frac{x}{r}$. The critical Reynolds Number $R_c$ of the transition from laminar to turbulent boundary layer on a flat sheet is a constant, other conditions being constant, but for a curved sheet it becomes a function of $\frac{x}{r}$. It ~~is~~ WAS the object of this research to determine the dependence of $R_c = \frac{Ux}{\nu}$ on $\frac{x}{r}$. The method of doing this was to make measurements at a point on the sheet; i.e. for a value of $\frac{x}{r}$, while varying the Reynolds Number by varying the speed U, until the transition was reached. A critical $R_c$ was thus obtained for a value of $\frac{x}{r}$. Similiar measurements were made at other points on the sheet, both on the concave and convex sides. By this method the critical Reynolds Numbers wereobtained for a series of values of $\frac{x}{r}$. The object of this discussion is to point out the fact that the effect of curvature on the critical Reynolds Number over a considerable range can be obtained with one radius of curvature. With the aid of a paper by Schlichting*, it was decided that a central sheet forty-eight inches long and

*Schlichting, H., Über die Entstehung der Turbulenz in einem Rotierenden Zylander, Gött. Nachrichten, Heft 2, pp. 160, 1932.

with a twenty inch radius of curvature would permit the measurement of critical Reynolds Numbers for a wide enough range of values of $\frac{x}{r}$.

In order to adjust the turbulence level of the free stream and measure the critical Reynolds Number for no curvature, a straight section similiar to the curved one was made. It is also planned to use this section to measure the effect of roughness on the transition.

When the tests were inaugurated, the straight section was initially used. The turbulence in the free stream, measured by means of a hot wire and amplifier* was found to be very high with frequent "bursts" that made the needle of the amplifier output meter go off the scale. This difficulty was obviated by putting sheets of plywood across the corners of the pressure box near the exit (see Fig. 1) where standing vortices were being formed and released into the stream. The result was a fairly steady reading indicating about one half of one percent turbulence in the free stream.

As the time was growing short all further tests on the straight section were deferred until next year and measurements were begun on the curved section. All tests on the straight section have been conducted by Mr. A. C. Charters.

*For details of the hot wire apparatus and technique see Appendix II.

MEASUREMENTS ON THE CURVED SECTION

From some work done by Dryden* it was seen that there was a point of maximum turbulence in the boundary layer near the transition. It was thought that it would be possible to utilize this phenomenon in locating the transition by placing a hot wire in the boundary layer and increasing the velocity until a point of maximum turbulence was reached.

However, when this work was begun the authors had no definite idea as to where a transition was to be expected, as the effect of curvature was unknown, and, also, no idea as to the optimum distance from the wall to place the hot wire. For this reason it was decided to make total head surveys at several points for a series of free-stream velocities in order to determine the character of the boundary layer. One set of these is plotted in Fig. 2. In this figure the ordinates were made dimensionless by dividing by the total pressure of the free stream. These measurements were made before the static pressure was adjusted to zero so that the curves were not converted to velocity profiles. The striking feature of these curves is that the free stream total pressure is reached at about the same distance from the wall independently of the free stream velocity. Only the shapes of the curves indicate a transition from laminar

*Dryden, H. L., Airflow in the Boundary Layer Near a Plate. N. A. C. A. Tech. Rep. No. 562, pp. 16, Fig. 22.

to turbulent boundary layer. It was here that appeared the first indication that the transition would be hard to define because of the gradual change from laminar to turbulent flow. However, these measurements did serve to indicate the range over which the transition could be expected, and the width of the boundary layer.

When the character of the flow had been tentatively established, the pressure gradient in the channel was adjusted to zero, and the static pressure $\frac{\partial T}{\partial}$ about a half of an inch from the wall was made equal to the atmospheric pressure. This was done by means of a tilting multiple manometer connected to small static tubes placed about every six inches around the plate. The final pressure variations were less than one percent of the dynamic pressure.

With the above data in mind, the output of a hot wire amplifier was connected to an oscillograph and visual and photographic measurements were made. These are shown in Figs. 3,4, 5, 6 . Fig.3 is a record taken in the free stream that indicates a fine scale turbulence which has a fairly uniform level. Fig.4 is a record of the turbulence in the laminar boundary layer. It is hardly turbulence in the usual connotation of the word, but is in reality comparatively slow variations which give a fairly large and very unsteady reading on the output meter. Fig. 5 is a record of the turbulence in the transition boundary layer. It comprises fluctuations similiar to those in the laminar layer and also fluctuations similiar to Fig. 6 which was made in the definitely turbulent boundary layer. It is practically impossible to read even a highly damped output meter when measure-

ments are being made in the transition region. From Fig.5 it is quite easy to see why the transition appears to be so gradual. The flow at the point of transition, being just on the verge of instability is markedly affected by any slight external disturbance. The variations in the free stream turbulence thus cause the point of transition to continually travel back and forth past the wire. This necessarily means that any measurements which tend to average the readings make the transition appear to extend over a large region. The meter readings for Fig. 6 were steady if a highly damped output meter was used.

In locating the transition by means of visual observations on the oscillograph, it was found impossible to make measurements which could be duplicated with any degree of occuracy. This led the authors to attempt making a series of turbulence profiles for various speed at several points. These profiles were taken at a point 100.2 cm. from the leading edge on the convex side of the sheet. The variations in Reynolds Number were obtained by changing the speed. These profiles are shown in Fig. 9 which are later crossplotted as equal turbulence level contours in Fig. 12. Next, additional profiles were taken at points 22.9 cms. and 36 cms. from the leading edge on the concave side of the sheet and are shown in Figs. 7, 8. On this side of the sheet these were the only two points at which it was possible to obtain measurements with the velocities

available without drilling more holes to admit the hot wire into the tunnel. After these profiles had been made, a great deal of difficulty was encountered with the hot wire apparatus, and after spending considerable time, further measurements of turbulence profiles were postponed until a later period.

It is interesting to compare the two turbulence profiles (Figs. 10, 11) for the concave side of the sheet with the one for the convex side and these in turn with the one given by Dryden which has been replotted in Fig. 13. All four show a point of maximum turbulence which may be taken as a characteristic point of the transition. The effect of curvature is to move the point of maximum turbulence closer to the sheet on the concave side and farther away on the convex side. After the transition the contour lines for the concave side move rapidly in toward the wall while on the convex side the lines appear to be drawn out in the direction of flow. Dryden's contours are not extended far enough to determine the character of this phenomenon for the straight wall. The peculiar swirls (see Fig. 10) in the contours for the convex side of the wall are due to the falling off of the profiles after a maximum had been reached and then suddenly rising again in the vicinity of the wall. This second rise was not noted on the concave side of the sheet.

The movement of the transition along the plate as shown by the three sets of contours taken by the authors are in the right direction and will be discussed more fully later. Dryden's contours indicate that the transition for his straight wall came at a later point than any of those given by the authors' curves. There are three factors which may have caused this

discrepancy: intensity and scale of turbulence in the free stream, and surface roughness of the sheet. The level of turbulence in Dryden's tunnel was given as 0.5% which is comparable to that in the authors' tunnel. The scales of turbulence in the authors' tunnel is unknown as no velocity correlations have been made as yet, and no value was given for Dryden's tunnel. Where Dryden used a polished aluminum sheet the authors used a rolled and polished steel sheet which had numerous small pits, evidently caused by the rolling. More data on the effect of this will be available when the contemplated roughness tests in the straight section are completed.

After the trouble with the hot-wire apparatus developed the authors decided that it might be possible to establish the transition by means of a series of equal velocity contours similar to the equal turbulence contours. The velocities were measured by means of a hot-wire anemometer which permitted measurements very close to the wall. A check run was made using a total head tube, and applying the wall correction obtained by Jones*, The results of both methods are shown in Fig. 14 for a point 100 cms. from the leading edge and at a speed of 18.5 meters per second. It was decided that the difference was not enough to warrant further investigation at this time. The more complete profiles are shown in Figs. 15-21. These were cross plotted as equal velocity contours in Figs. 22-26. If we compare these

*Jones, B.M., Measurements of Profile Drag by Pitot Traverse Method, R & M 1688.

we see that the effect of curvature is to increase the boundary layer thickness on the convex side of the sheet and to decrease it on the concave side for both the laminar and the turbulent boundary layer. This is in accord with the measurements made by Wattendorf* in a fully developed turbulent flow. Very unfortunately there is no characteristic feature of these contours which can be used in definitely defining a transition.

By this time the hot-wire apparatus had been restored to working order but as the time was growing short, it was decided for the present not to complete the turbulence contours. However, if we examine the contours already completed we see that it would be a comparatively easy matter to locate the maximum points. The operating technique was as follows: From the turbulence profiles already taken, the distance from the wall at which the point of maximum turbulence would occur could be estimated. With the hot-wire in this position, the speed was incresed, both the x and y-Reynolds Numbers proportionately corresponding to a traverse along a line through the origin of a diagram similiar to Figs. 10-13 . As the speed was increased a maximum value of turbulence was observed. The wire was then moved in and out until another maximum was observed, and with wire in new position the first operation was again repeated. This is a rapidly convergent process, the final maximum being usually located at the end of the second trial.

*Ibid, pp. 576, Fig. 9.

The final results are shown in Fig. 27 . These curves were obtained by making turbulence readings at a series of velocities with the hot-wire in the final position.

Before entering into a discussion of these results it is perhaps best to see what effect the curvature might be expected to be. In order to do this we go back to the equations of motion for curved potential flow.

$$\frac{\partial p}{\partial r} = \rho \frac{u^2}{r} - \rho \frac{u}{r} \frac{\partial v}{\partial \theta}$$

For our case the second term may be considered to be zero,

$$\therefore \frac{dp}{dr} = \rho \frac{u^2}{r} \qquad (1.)$$

which means that the centrifugal force $\rho \frac{u^2}{r}$ just balances the radial pressure gradient.

Since the vorticity is zero, $\frac{d}{dr}(ur)$. The following sketch shows this velocity distribution and the velocity distributions on both sides of the sheet in the region of the boundary layer.

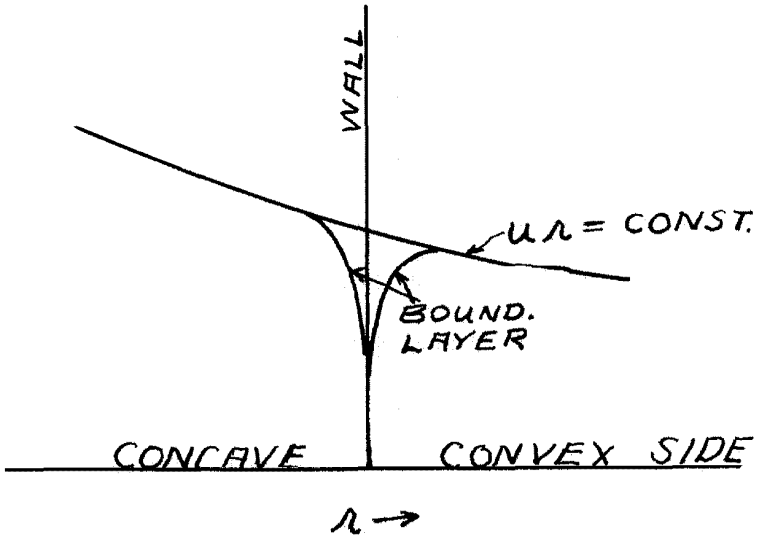

On the concave side of the sheet $\frac{d}{dr}(ur)<0$ and on the convex side $\frac{d}{dr}(ur)>0$. Let us first consider what happens to a particle on the concave side when it is displaced from its path. If it is displaced outward (i.e. into boundary layer) it will have a velocity $u \simeq \frac{u_0 r}{R}$ which is greater than that of its surroundings. This means that the centrifugal force $\rho \frac{u^2}{R}$ is greater on this particle than on the surrounding particles. and hence the particle is thrown farther outward. Similarly, if the particle is displaced inward. If a particle on the convex side of the sheet is displaced outward it has a lower velocity and consequently lower centifugal force acting on it than the surrounding particle. Thus it tends to go back to its original position. A similiar thing would happen if it were displaced inward. Consequently disturbances on the concave side of the sheet tend to be amplified and disturbances on the convex side tend to be damped out. This leads us to the conclusion that the effect of curvature will be to precipitate the transition at an earlier point on the concave side and prolong it to a later point on the convex side. From Fig.27 we see that this is exactly what happens. For the concave side of the sheet, the maximum point of the turbulence curves is shifted to the left for increasing values of $\frac{x}{r}$, and for the convex side the curves are shifted to the right for increasing values of $\frac{x}{r}$. The experimental points for $\frac{x}{r}$= 2.25 and $\frac{x}{r}$ =1.975 are quite scattered and appear to lie on the same curve. The scatter is due to the low speeds at which it necessary to run these test. At these speeds all frequencies are correspondingly lower which results in a very unsteady reading on the output meter. If it is possible to get an even more

highly damped meter more accurate results may be obtained which will show a separation of these curves. As was mentioned previously, the turbulence drops off rapidly after the transition is reached on the concave side, but is maintained for some distance on the convex side. Thus there is liable to be some ambiguity in defining a transition. Two definitions have been taken, one being the point where the maximum is first reached, and the other where the turbulence is 95% of its maximum value. The first is rather indefinite for points on the convex side, as here the maximum is reached rather slowly. The second is more concise as it comes at about the place where the curves start to level off.

Using both definitions, critical Reynolds Numbers have been plotted as a function of $\frac{x}{r}$ in Fig.28. In absence of any further information two straight lines have been faired through the points. The two sets of points for the two sides of the sheet are surprisingly consistent. It can be seen from the curve that the critical Reynolds Number for a straight sheet turns out to be about $4 \times 10^5$. This agrees with results obtained by van der Hegge Zijnen but is lower than the values obtained by Dryden. Some of the possible causes for disagreement with Dryden's work were discussed earlier in the paper. When the straight section of the present tunnel is installed in the future, more data will be available on this point.

## CONCLUSION

So far the chief object of this work has been to build the tunnel and put it in proper working order. As yet no extensive series of measurements have been undertaken, the object of the authors being to try to determine what methods of proceedure lead to the most practical and consistent set of results. As in all research work, a great many difficulties were encountered. For the most part these have been successfully overcome and it is hoped that the work in the future will proceed with a minimum of trouble and hard luck.

## Appendix I Detailed Description of the Various Parts of the Channel.

### FAN (See photos 1,2)

The fan was designed with the aid of a report by Kellar.* The outside diameter was forty inches and the hub diameter was twenty-four inches. It has eight wooden blades, mounted adjustably in a steel hub and is driven by means of two V-belts from a twelve and one half horsepower direct current motor which is located below the fan casing. The hub fairing was extended out in front of the tunnel about 2 feet to save making an expensive hub fairing. A counter propellor consisting of eight sheet metal blades, (not shown in the photographs) was placed in front of the propellor, serves to eliminate the rotary component of velocity induced by the propellor. At a maximum of 1500 R. P. M., the fan was designed to give a velocity of from 80 to 90 feet per second in the working section. Velocities as high as 83 feet persecond have been obtained.

### DIFFUSER (See photos 3,4)

The diffuser is 16½ feet long and made of riveted twenty gauge galvanized iron sheets. It consists of an external truncated cone with a minimum diameter of 40 inches, a maximum diameter of 56 inches, and an inner cylinder with a diameter of 24 inches. This latter serves as an extension for the hub. This arrangement was chosen when it proved to be the cheapest of three different designs to construct. It has an expansion ratio of 2½ to 1 .

*Kellar, C. Axialgebläse vom Standpunkt der Tragflügeltheorie, Mitteilung aus dem Institut für Aerodynamik. Eidgenössische Technische Hochschule, Zürich.

Thus 84% of the dynamic head is converted into static pressure before entering the box.

PRESSURE BOX

This box was originally designed to be used on an open circuit, open jet tunnel which has since been made into a close circuit tunnel. The frame-work is made of 2" x 2" angles and I beams. The covering consists of sheets of one inch plywood, bolted on, and sealed with red lead to prevent leaks. All three of its diminsions are 7 feet. An extensive series of tests was undertaken to make the turbulence level at the exit of the box a minimum. The final arrangement consists of two screens to damp out the eddies of the propellor, and plywood fairings across the corners near the exit (See Fig. 1 ). One of the screens was made of two layers of cheese cloth and one layer of common copper window screening; the other was made of five layers of cheese cloth. These seemed to give a very uniform steady flow across the whole cross section of the box. The plywood fairings served to eliminate standing vortices in the corners of the box.

WORKING SECTION (See photos 5,6)

The straight and curved working sections are very similar, as few modifications were necessary to accomodate the curvature to the straight section. The main part of both is the central 20 gauge polished steel sheet which is clamped between 2" x 3" angles at the ends. These angles are bolted to the external frame-work (See photo 7 ) in such a way as to put up to 100 pounds per running inch tension into the sheet

in order to hold it in shape and keep it from vibrating. The side walls were stiffened with vertical 1" x 1" angles connected at the top and bottom to the 2" x 3" angles by means of threaded 3/8" studs. The distance between the side walls and the center sheet was adjusted by means of the studs which moved the stiffners in or out. The leading edge of the central sheet was sharpened with a taper that extended back about an inch.

Measuring apparatus such as pitot tubes and hot-wires were admitted through holes in the outer walls and extended across to the central wall. These were mounted on a micrometer screw carriage on a separate stand (See photo 8 ).

EXIT DIFFUSER (See photo 9 )

The exit diffuser was simply added to reduce the exit velocity of the air to a point where it would not create undesirable eddies in the surrounding room. It was made of 3/4" plywood mounted on a very simple frame-work. The divergence angle was $12\frac{1}{2}^{0}$. In order to overcome the pressure rise due to this divergence, two screens were placed in the diffuser. These screens were adjusted until atmospheric pressure was approximately obtained. The final adjustment was made by means of shutters at the opening.

## Appendix II•HOT-WIRE APPARATUS AND TECHNIQUE.

Hot-wire research illustrates the typical difficulties that are encountered in almost any kind of research work. When one is first initiated into the mysterious order of the compensating resistance and time constant one is deeply impressed with the inconsistencies of the whole procedure. For example, hot-wires are compensated for frequency response to within 2 or 3%, and yet the frequency response of the amplifier is not constant to within 50%, as the gain falls off very rapidly at low frequencies. However, one soon learns to accept this as part of the by-laws and to go about one's duties without heed or complaint.

### PREPARING THE HOT-WIRES

The hot-wires are made of .001 in. Wollaston wire which is a .0001 in. platinum wire with a .0009 in. silver covering. The wire was soldered to the holder by means of soft solder. In using plain platinum wire, trouble had been experienced with poor connections when soft solder was used, but the silver coating on the Wollaston wire gave a very good bond. After the wire was soldered in place about a half or three-quarters of a millimeter of silver in the center was etched off by means of a bubble of concentrated nitric acid formed at the end of a capillary tube.

In soldering the wires, a few valuable points of technique were discovered. Best results are obtained in both the soldering and etching processes if the wire and spindles are kept as clean as possible. It may take as long as an hour

for the acid to eat through a thin film of grease on the wire. While soldering, the spindles are sprung slightly apart so when released the wire will have a slight curvature which gives it flexibility. Immediately after releasing the spindle the wire bends sharply in the middle. This sharp bend is removed by letting the wire carry the entire weight of the spindles and support on the end of a pencil. When the wire has a very gentle bow in it, the spindles are gently heated with a soldering iron to relieve any residual stresses in the wire, which after etching are transferred to the etched portion, causing it to take all kinds of queer shapes. If the finished wire has the shape shown in the following sketch, it will stand a lot of comparatively hard usage.

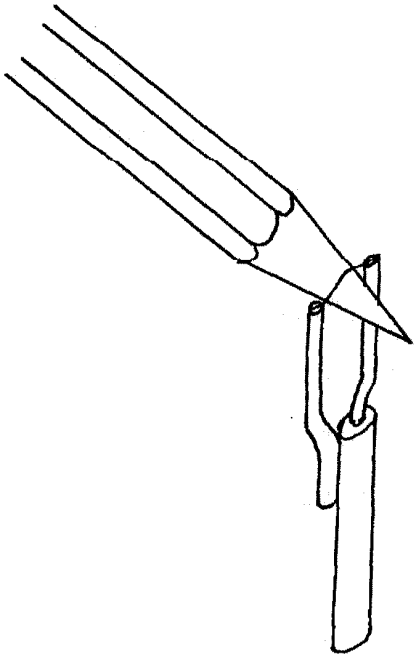

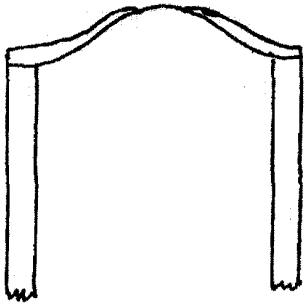

OPERATION OF THE AMPLIFIER(See photo 10)

The amplifier is of standard design (for diagram of the circuit see Fig. 29 ). The four stages, with resistance coupling between stages, gives a total gain of about 240,000. The gain if maintained at a constant value by means of an altenuater and a standard input voltage. Due to insufficient coupling the amplifier falls off in gain very rapidly below 100 cycles per second. Above 100 cycles, the increase in gain with frequency proved to be just about suffieient to compensate for the distorted frequency response of the very fine Wollaston wire which normally requires only a very small amount of compensation. The amplifier had originally been built with a variable unit to compensate a plain platinum wire/which, because of its larger diameter, needs a much higher degree of compensation. For this reason a low enough value could not be obtained to exactly compensate the Wollaston wire. For this reason, these tests were run without any frequency compensation other than that given automatically by the amplifier.

METHOD OF CALIBRATING HOT-WIRES

Two calibration are necessary for a hot-wire; the first is the calibration of the resistance against the mean velocity when the wire is used as an anemometer, the second is the calibration of the reading of the output meter of the amplifier against the fluctuating velocity at the wire when it is used to measure the level of turbulence. The first calibration is comparatively simple. The resistance of the wire is measured by means of a Wheatstone bridge at a series of

known velocities and a curve faired through the experimental points. A typical curve is given in Fig. 30.

A special tunnel has been designed and made by F. D. Knoblock of the Guggenheim Aeronautics Laboratory for the turbulence calibrations. In this tunnel, the hot-wire and holder are vibrated by means of a taut three wire suspension. This system is energized by a magnetic pick up and vacuum tube amplifier. The frequency is varied by tightening the suspension and measured by an oscillograph and oscillator. The amplitude of vibration is measured by means of a telescope and cross-hairs mounted on a micrometer carriage.

The usual procedure in calibrating a wire was to set the frequency at say 140 cycles per second, the amplitude at say 6mm., and the static pressure (which has been calibrated against a pitot tube) at say 25cm. of alcohol. The output meter is then read. Similar calibrations were usually made at a series of tunnel velocities.

This calibration really gives the output reading corresponding to a calculable level of (artificial) turbulence whose amplitude has the form $\Delta = \frac{\Delta_0}{2} \sin 2\pi\omega t$ where $\Delta_0$ is the double amplitude and $\omega$ is the frequency. The calculation of the level of turbulence is as follows.

$$\%\text{turb.} = \frac{u'}{U} \times 100$$

where $u'$ is average value of the fluctuating velocity,
U=mean velocity at the wire.

Now $u' = \sqrt{\overline{u^2}} = \sqrt{\overline{\left(\frac{d\Delta}{dt}\right)^2}}$

Also $\frac{d\Delta}{dt} = \pi\omega\Delta_0 \cos 2\pi\omega t$

and $\therefore u' = \sqrt{\frac{\int_0^t u^2 dt}{t_0}} = \pi \omega \Delta_0 \sqrt{\frac{\int_0^{\frac{1}{\omega}} \cos^2 2\pi\omega t \, dt}{\frac{1}{\omega}}}$

$$= \frac{\pi}{\sqrt{2}} \omega \Delta_0$$

Also $$u = \sqrt{\frac{2k\gamma P_s}{\rho}}$$

where k is the constant of calibration of static pressure against dynamic head = .860.
$\gamma$ = density of alcohol
$P_s$ = static pressure of tunnel
$\rho$ density of air.

$$\therefore \text{ \% turbulence } = \frac{\frac{\pi}{\sqrt{2}} \omega \Delta_0 \times 100}{\sqrt{\frac{2k\gamma P_s}{\rho}}}$$

which corresponds to a meter reading of $I_0$. For any other meter reading I, the turbulence level is:

$$\text{\% turb.} = \frac{I}{I_0} \frac{\pi \omega \Delta_0 \times 100}{2\sqrt{\frac{k\gamma P_s}{\rho}}}$$

HEAT LOSS DUE PRESENCE OF WALL

After reading a comment by Dryden*, who expressed the belief that sufficient knowledge was not available to formulate a heat loss correction which meant anything, no such correction was applied.

*Dryden, Ibid. p.10.

FIG. 1.

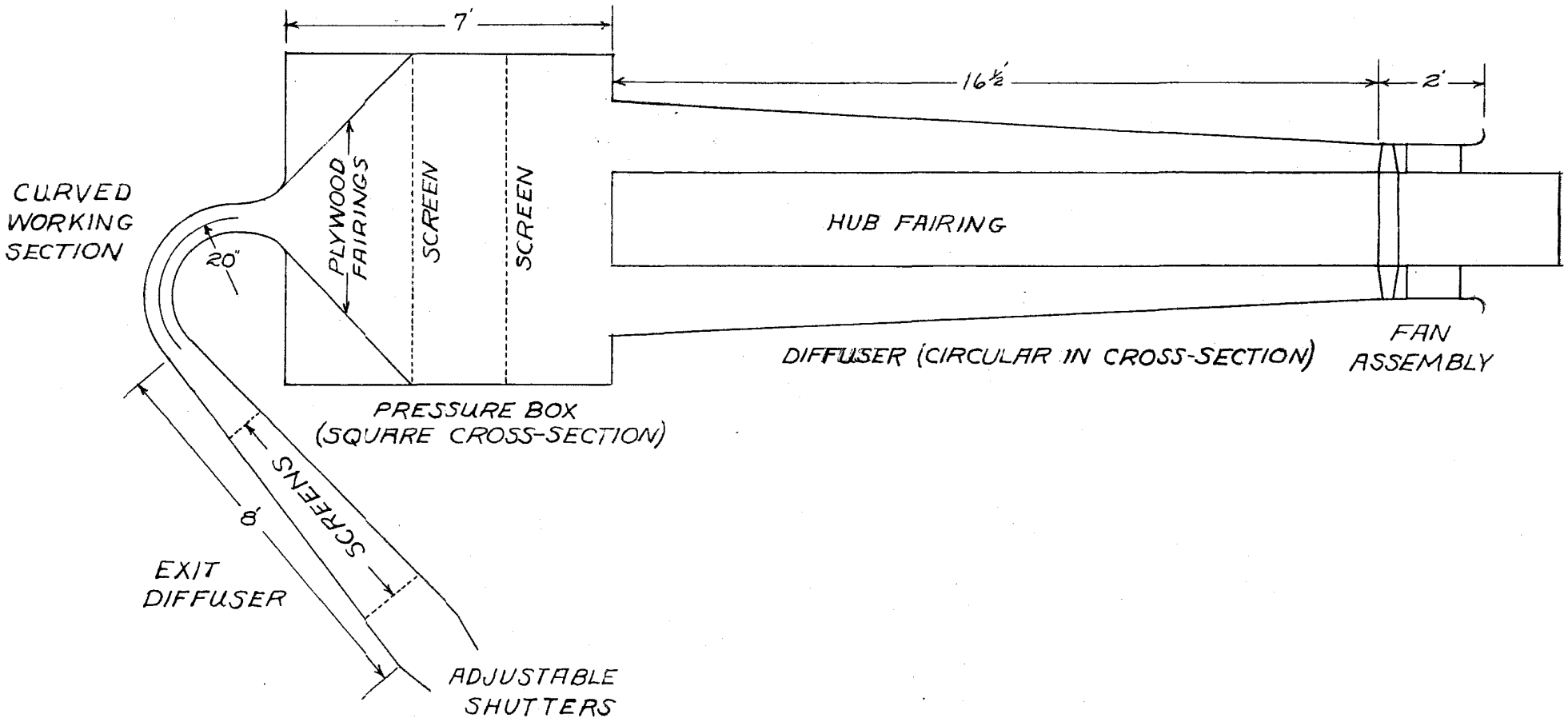


DIAGRAMATIC SKETCH OF TUNNEL ASSEMBLY. PLAN VIEW.

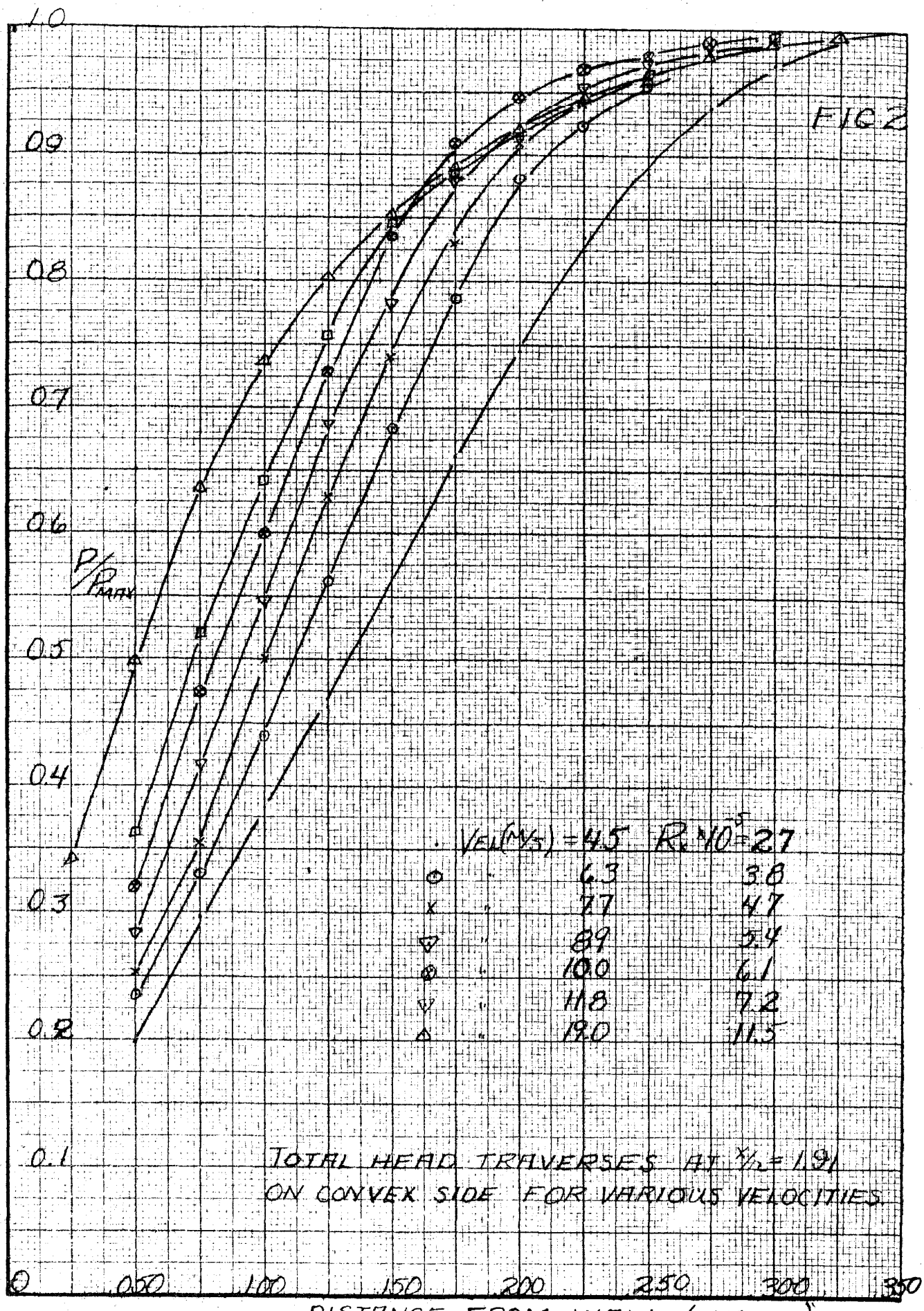
FIG 2
1.0
0.9
0.8
0.7
0.6
P/P_MAX
0.5
0.4
0.3
0.2
0.1
0
050
100
150
200
250
300
350
DISTANCE FROM WALL (INCHES)
VEL(M/S) = 4.5 R_x 10^-5 = 2.7
6.3 3.8
7.7 4.7
8.9 5.4
10.0 6.1
11.8 7.2
19.0 11.5
TOTAL HEAD TRAVERSES AT X/L = 1.91
ON CONVEX SIDE FOR VARIOUS VELOCITIES

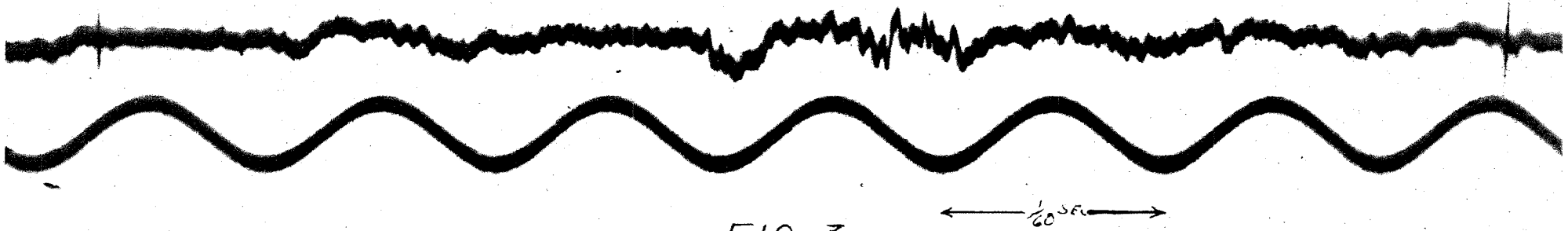


FIG. 3

OSCILLOGRAPHIC RECORD OF TURBULENCE IN THE FREE-STREAM

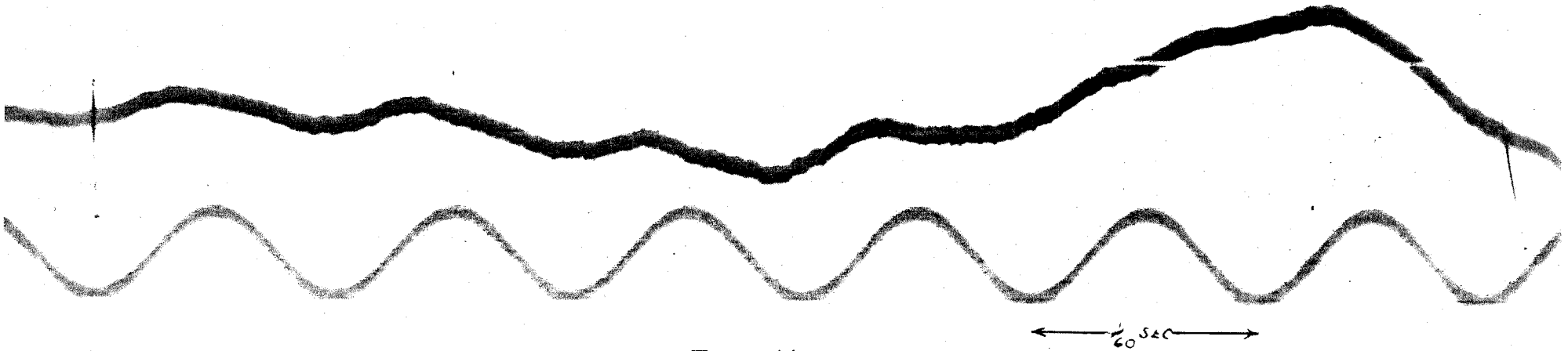


FIG. 4

OSCILLOGRAPHIC RECORD OF TURBULENCE IN LAMINAR BOUNDARY LAYER

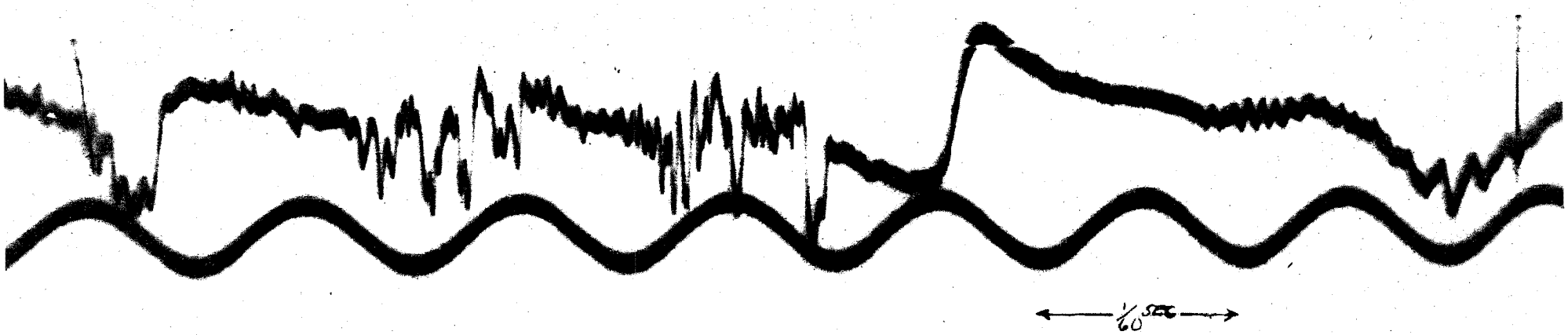


FIG. 5

OSCILLOGRAPHIC RECORD OF TURBULENCE IN TRANSITION BOUNDARY LAYER

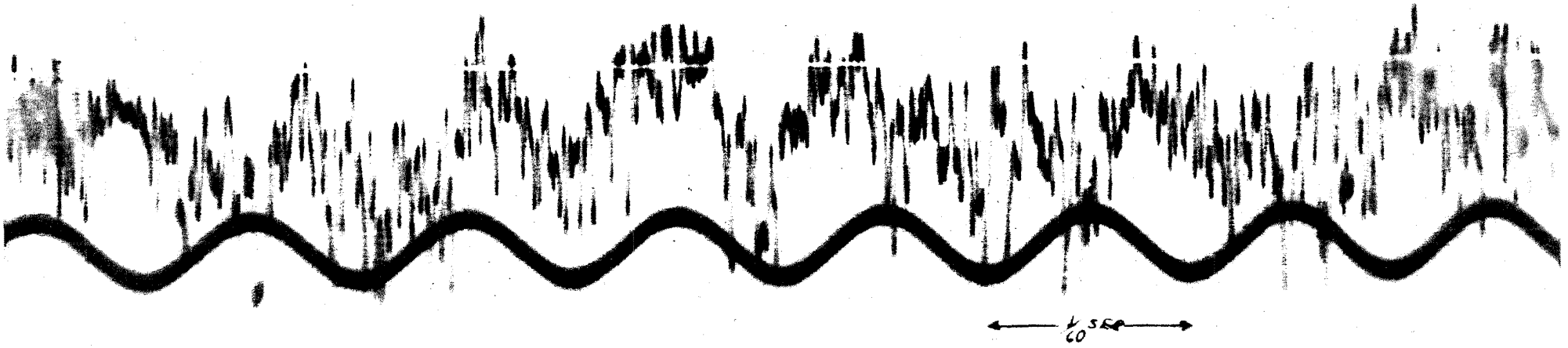


FIG. 6

OSCILLOGRAPHIC RECORD OF TURBULENCE IN TURBULENT BOUND. LAYER

FIG 7

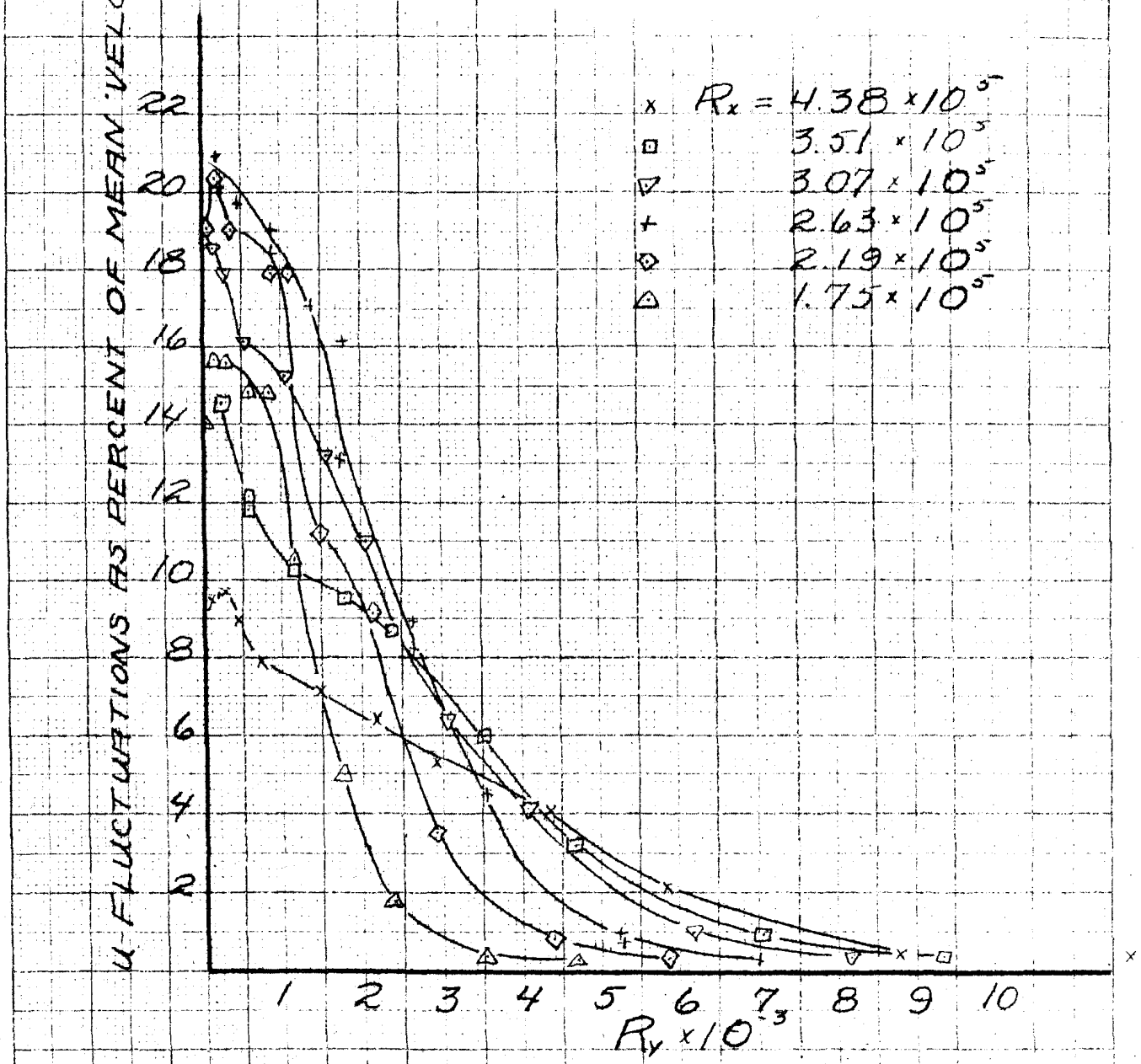


TURBULENCE LEVEL PROFILES $X/L = .748$
CONCAVE

FIG. 8

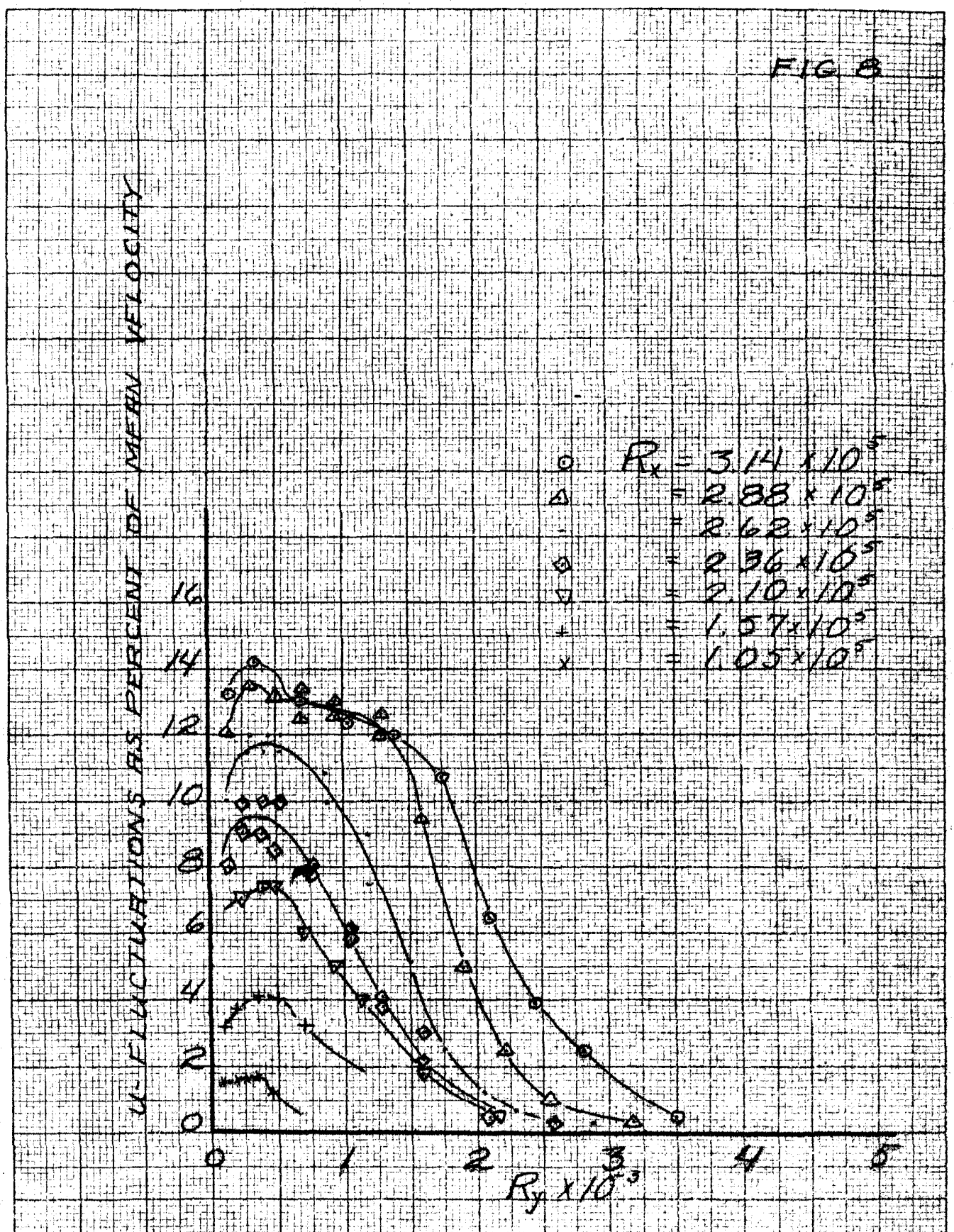


TURBULENCE LEVEL PROFILES $x/L = .437$
CONCAVE

FIG 9

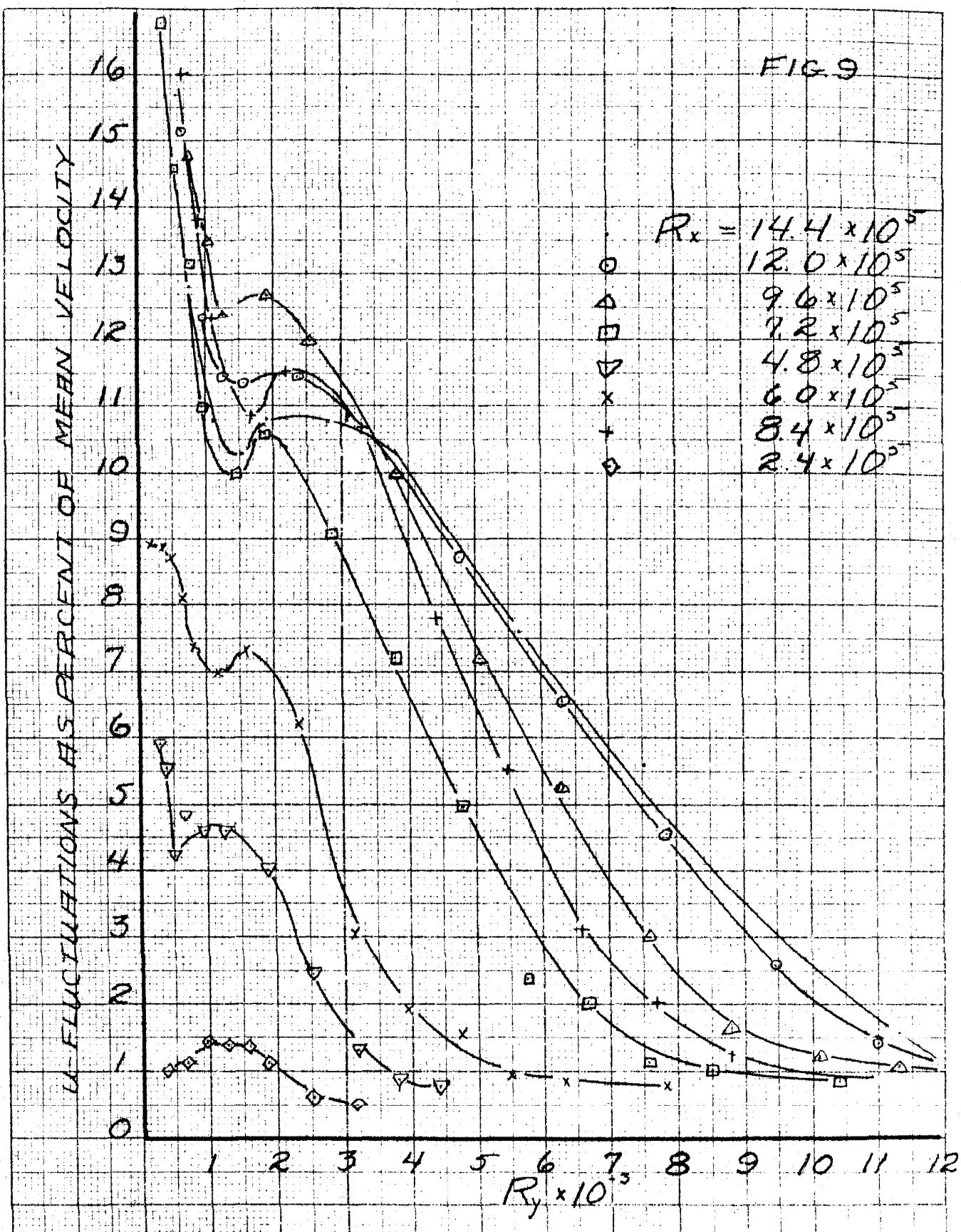


TURBULENCE LEVEL PROFILES $x/h = 1.975$

CONVEX

FIG 10

CONTOURS GIVE u-FLUCTUATIONS AS PERCENTS OF MEAN VELOCITY. CROSS-PLOT OF FIG 7

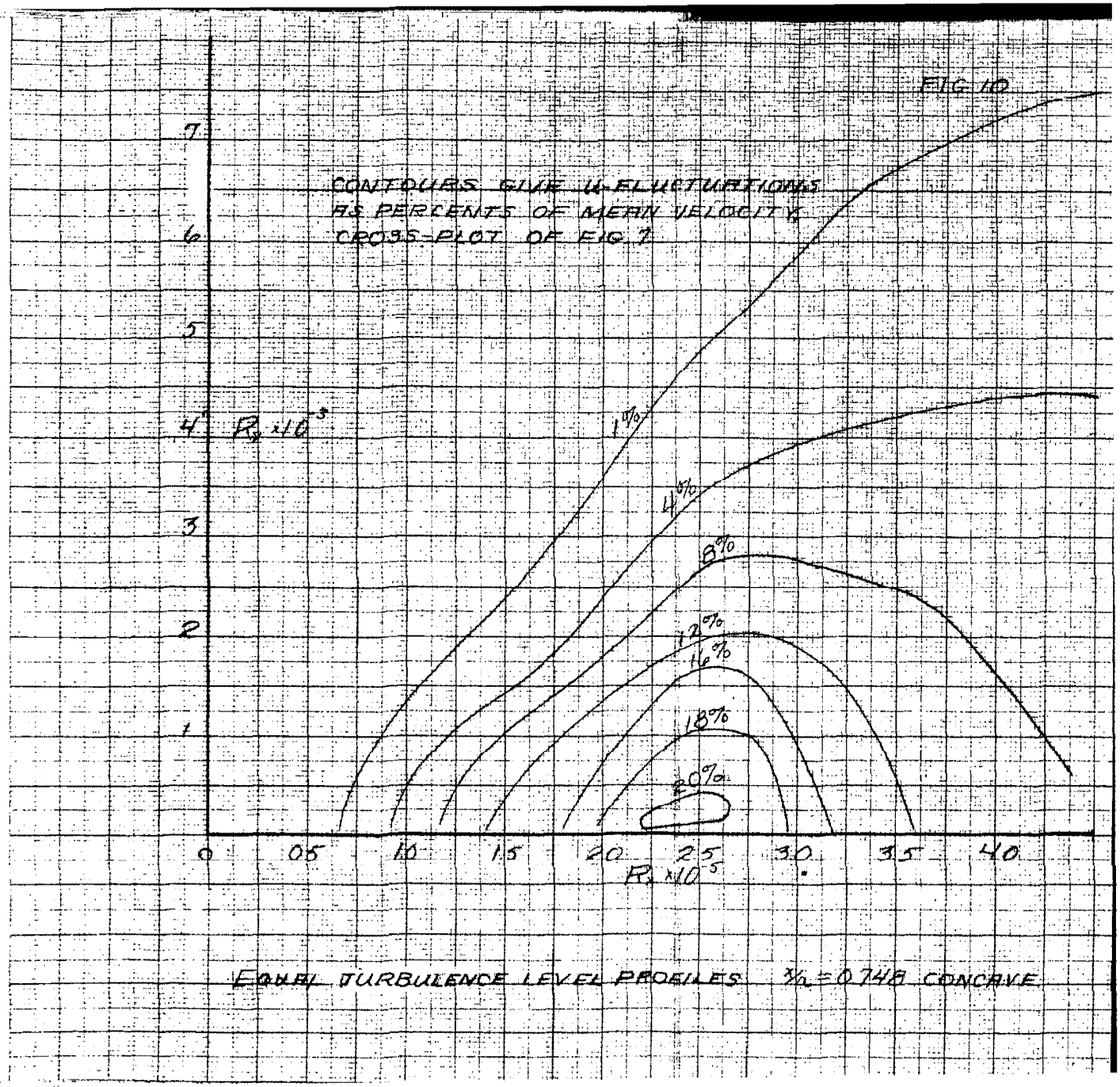


EQUAL TURBULENCE LEVEL PROFILES $x_0 = 0.748$ CONCAVE

FIG. 11

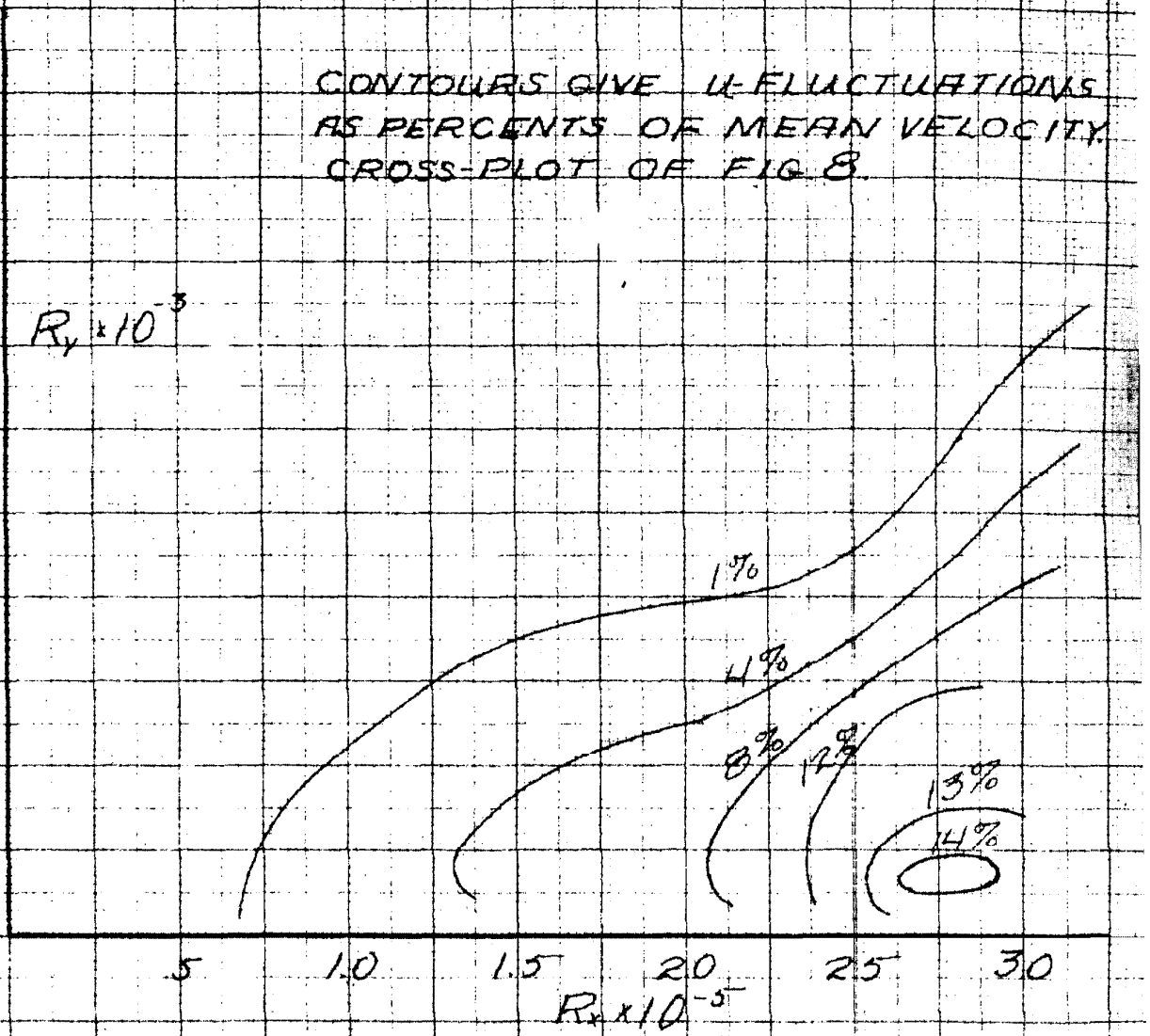


EQUAL TURBULENCE LEVEL CONTOURS

$x/L = 0.451$ CONCAVE

FIG 12

CONTOURS GIVE u-FLUCTUATIONS AS PERCENT OF MEAN VELOCITY. CROSS-PLOT OF FIG. 9

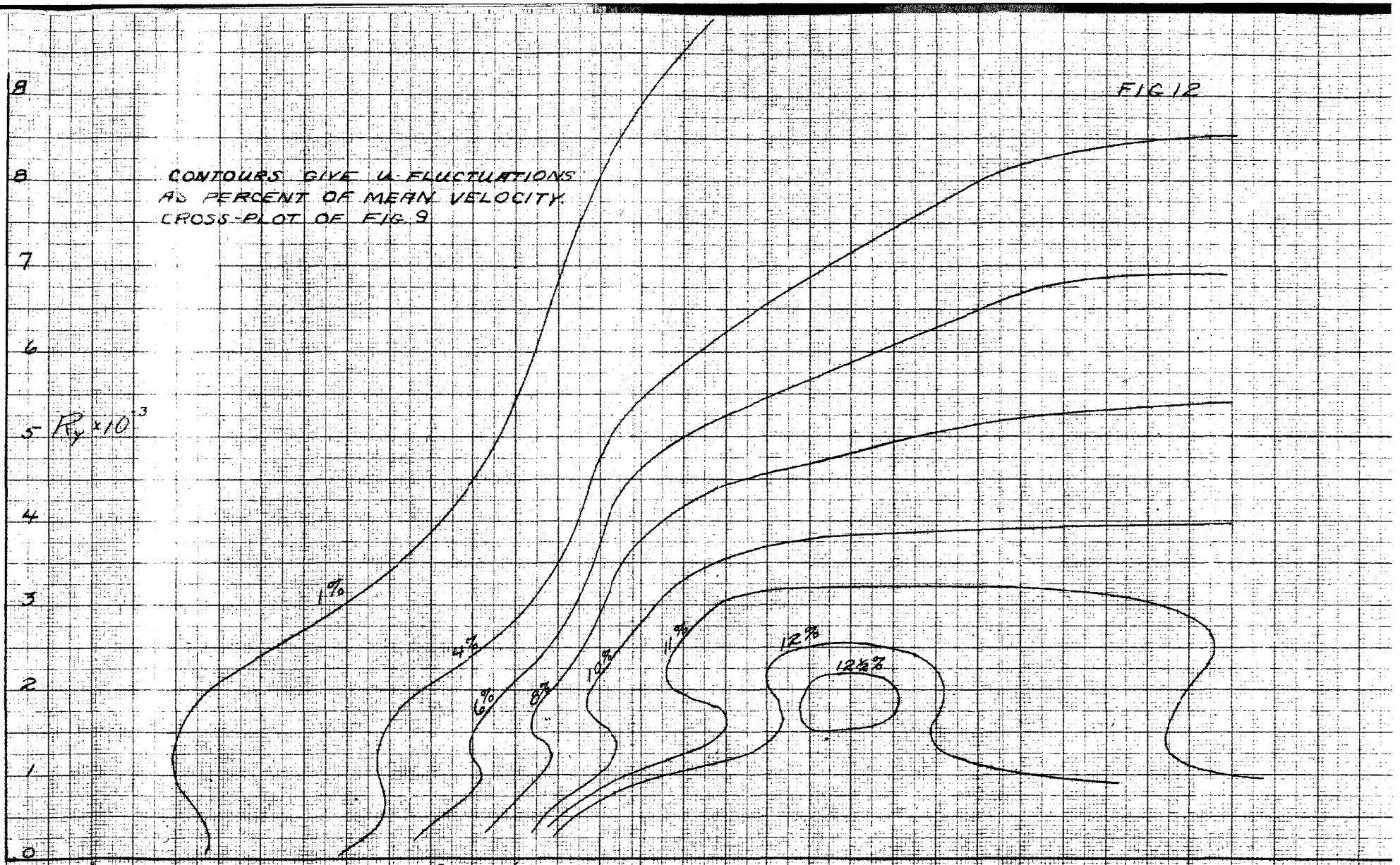


EQUAL TURBULENCE LEVEL CONTOURS $X_{in} = 1.975$ CONVEX

FIG 13

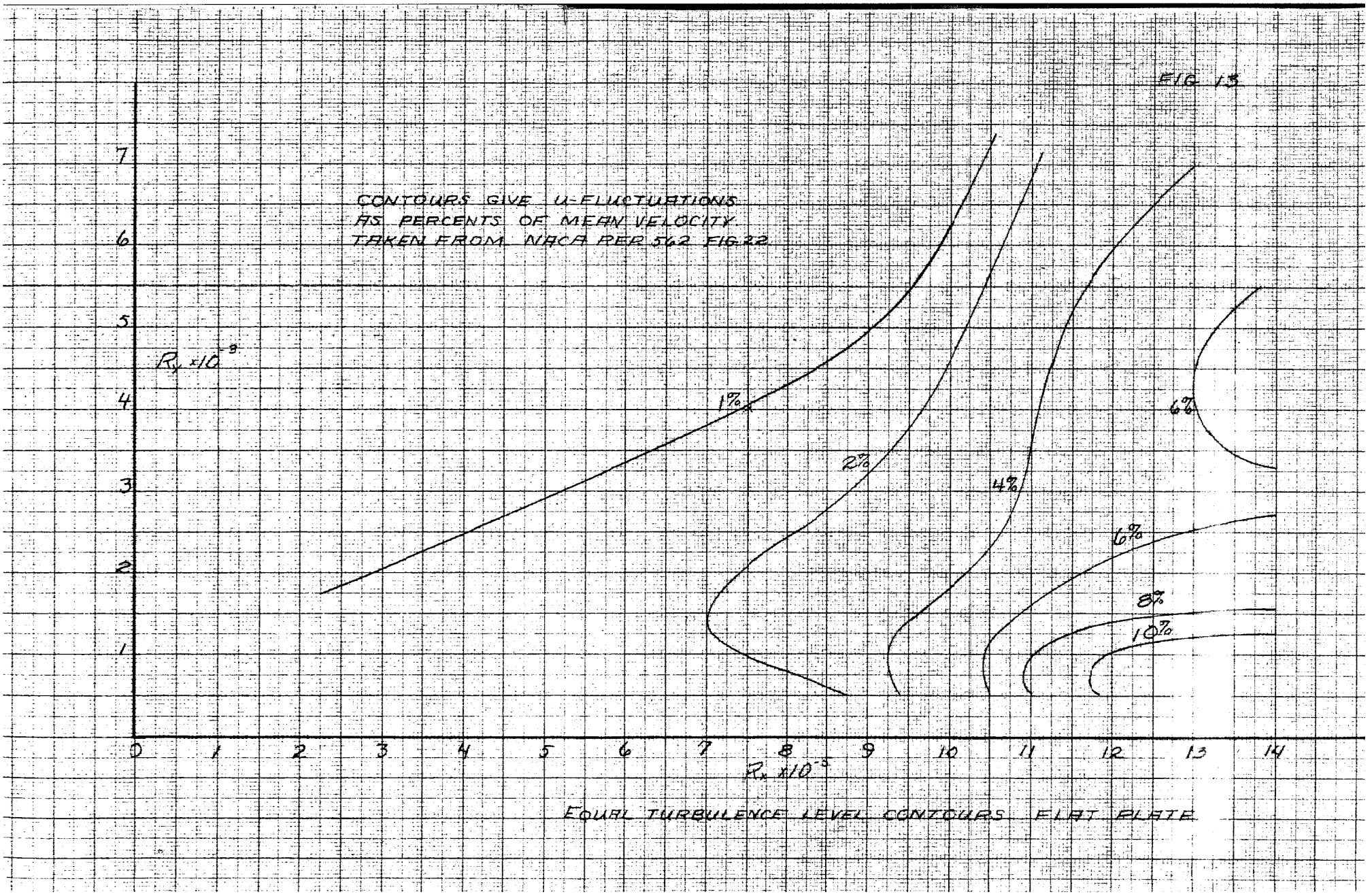


EQUAL TURBULENCE LEVEL CONTOURS FLAT PLATE

FIG. 14

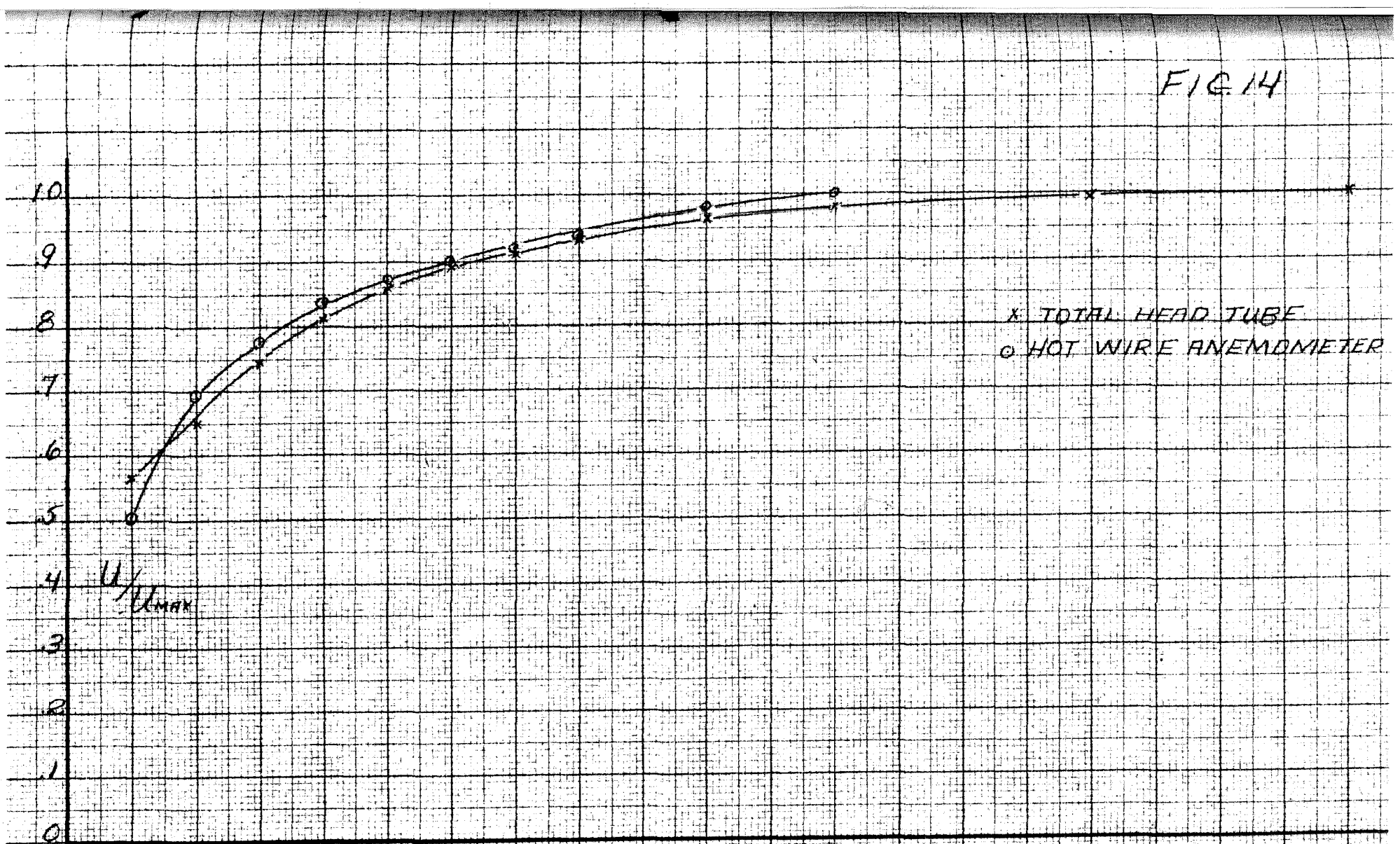


COMPARISON OF VELOCITY TRAVERSE TAKEN WITH TOTAL HEAD TUBE AND HOT-WIRE ANEMOMETER

FIG 15

MEAN VELOCITY PROFILES

$\frac{x}{h} = 0.498$ CONCAVE SIDE

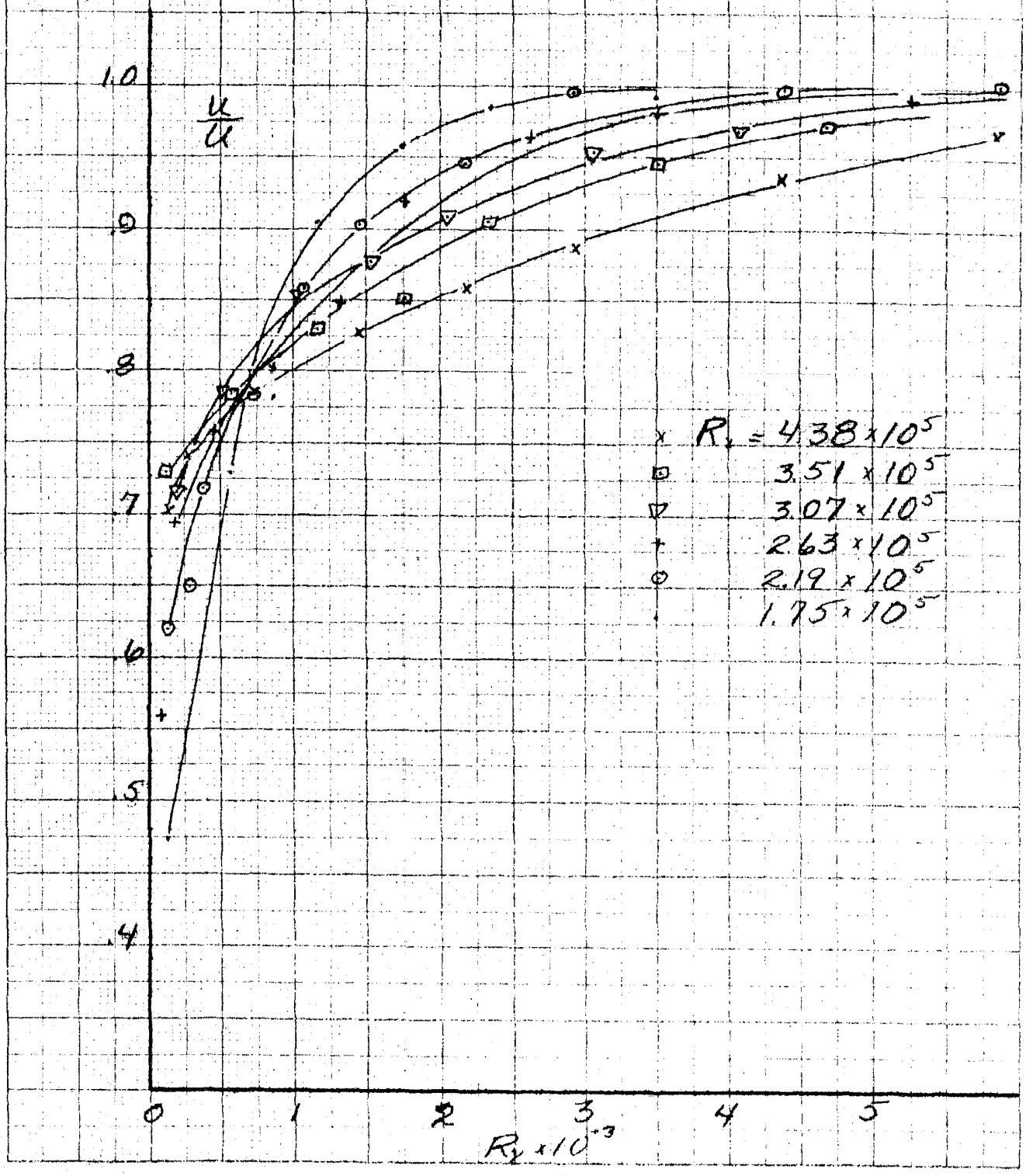

FIG 16

MEAN VELOCITY PROFILES

$x/n = 1.348$ CONVEX SIDE

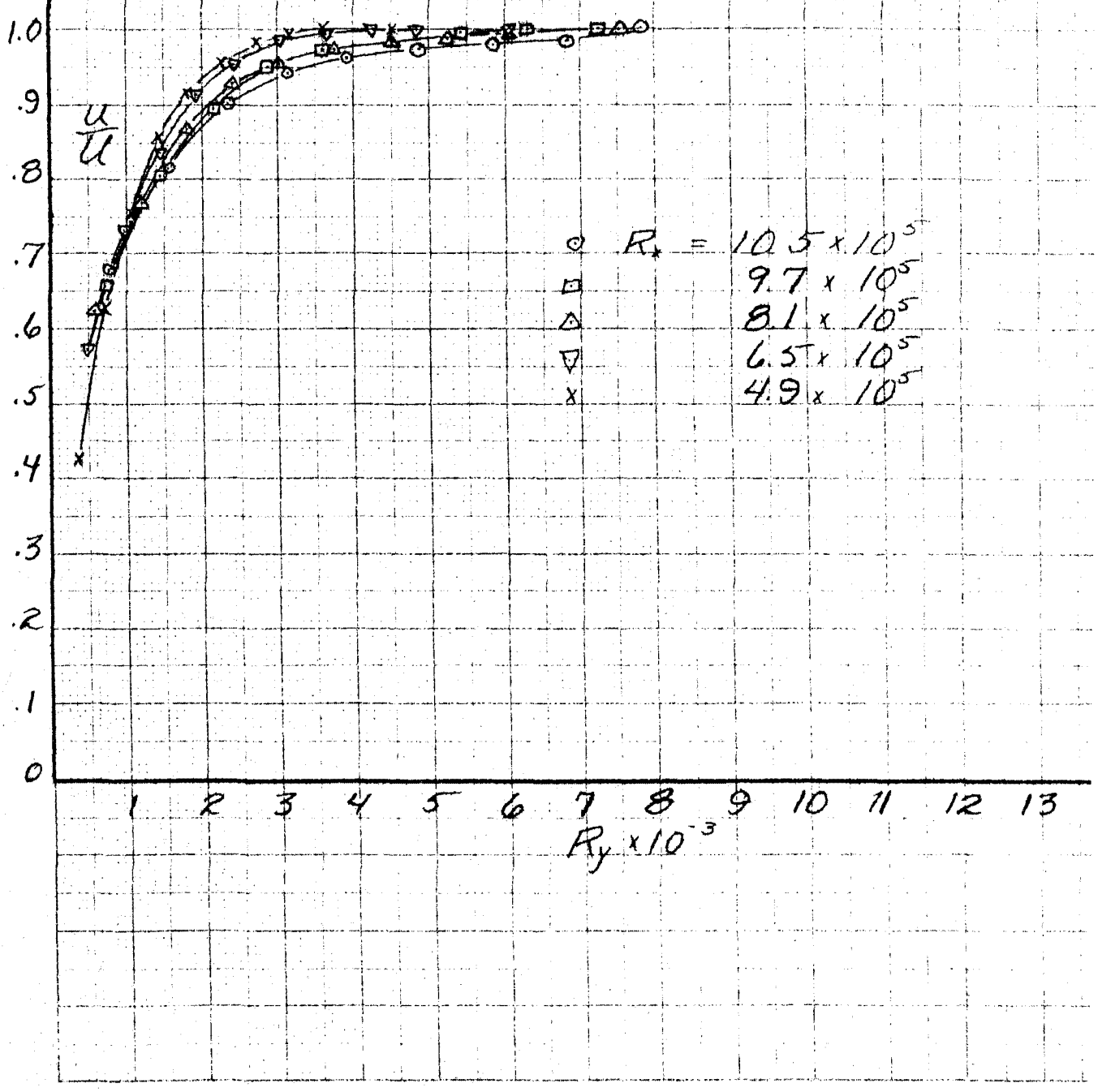

FIG 17

MEAN VELOCITY PROFILES

$x/R = 1.652$ CONVEX SIDE

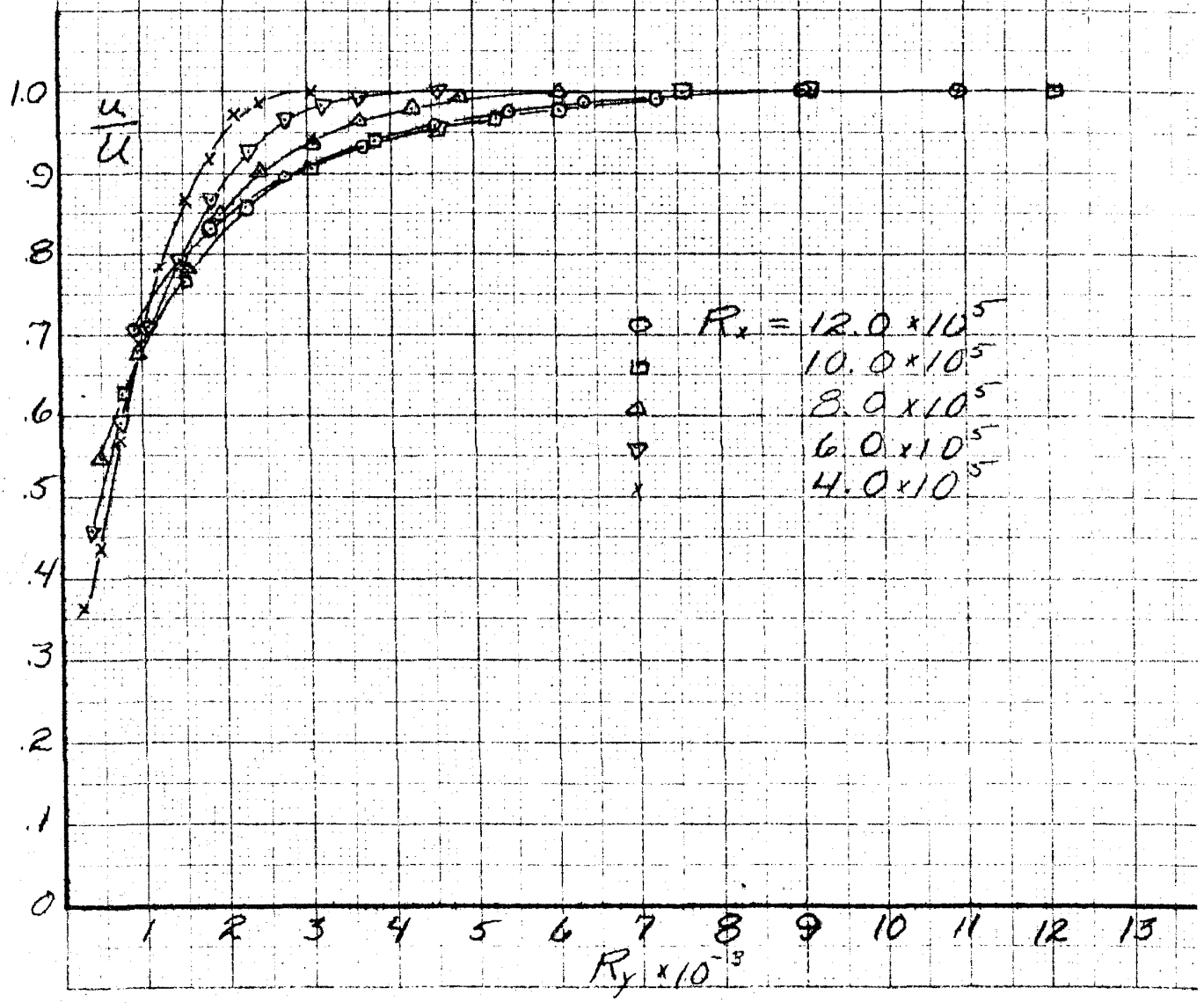

FIG 18

MEAN VELOCITY PROFILES

$x/r = 1.975$ CONVEX SIDE

RUN 2

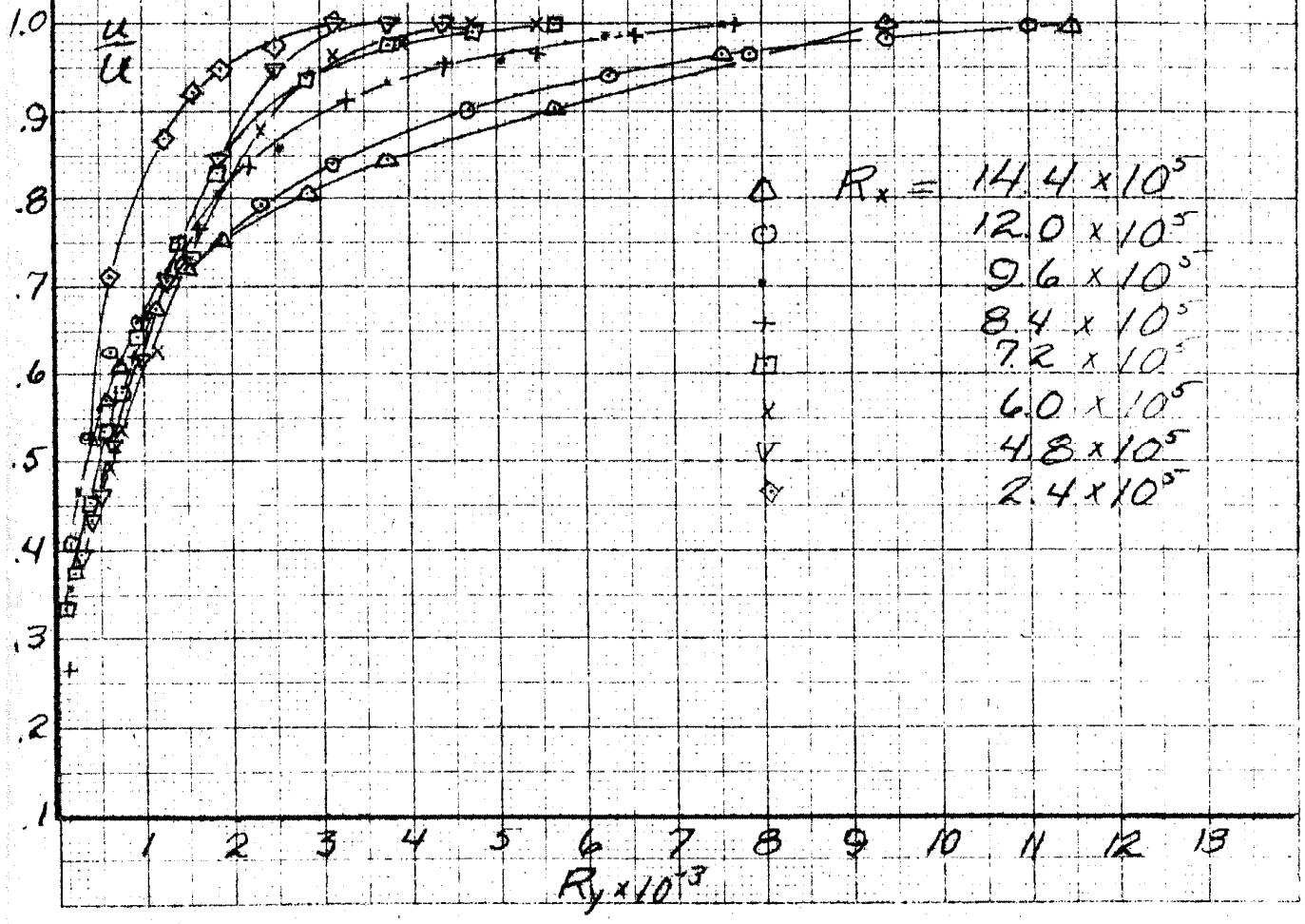

FIG 19

MEAN VELOCITY PROFILES

$x/R = 1.975$ CONVEX SIDE

RUN 9

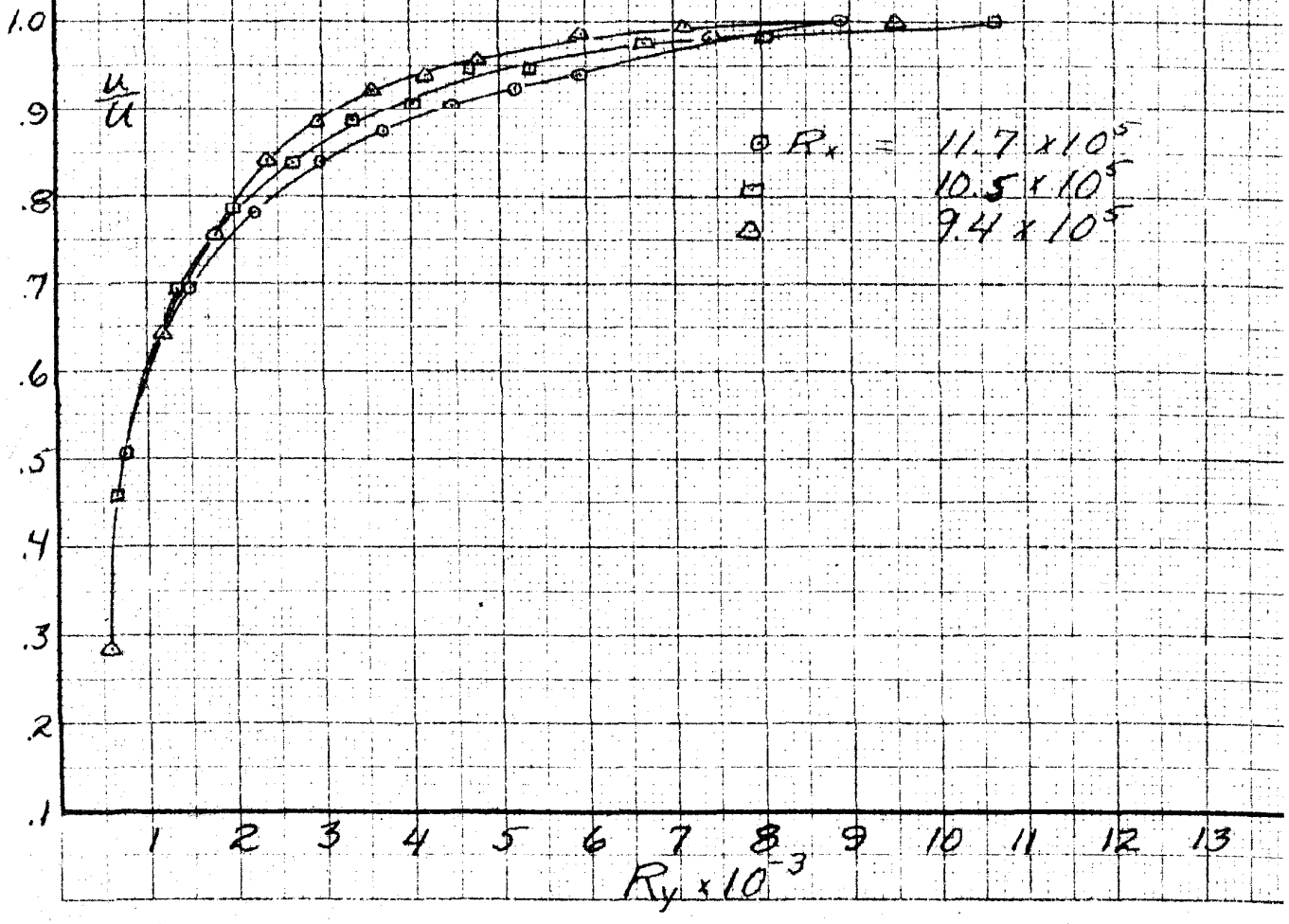

FIG 20

VELOCITY PROFILES

$x/h = 1.975$ CONVEX SIDE

RUN 7

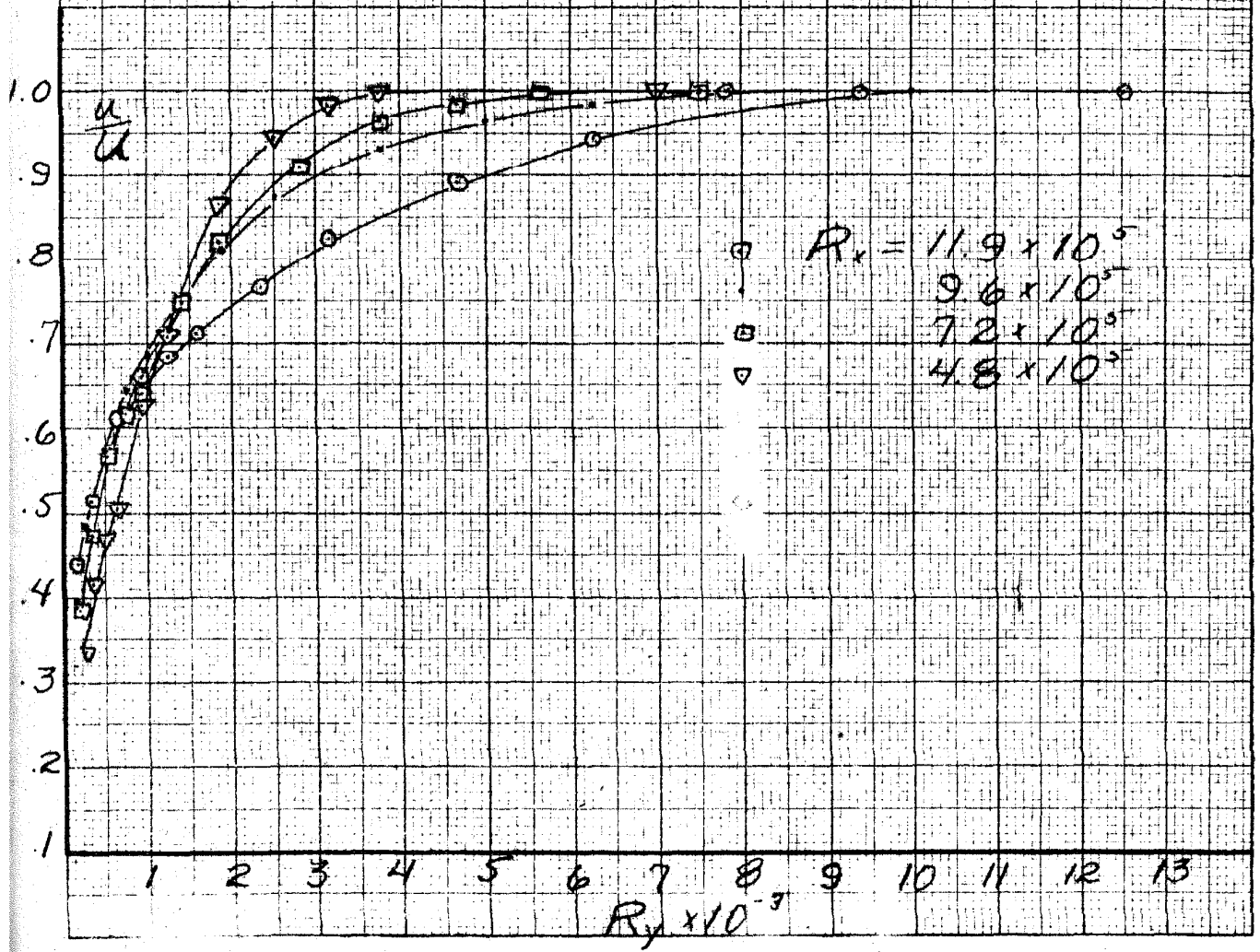

FIG 21

# MEAN VELOCITY PROFILES

## $Y/h = 2.250$ CONVEX SIDE

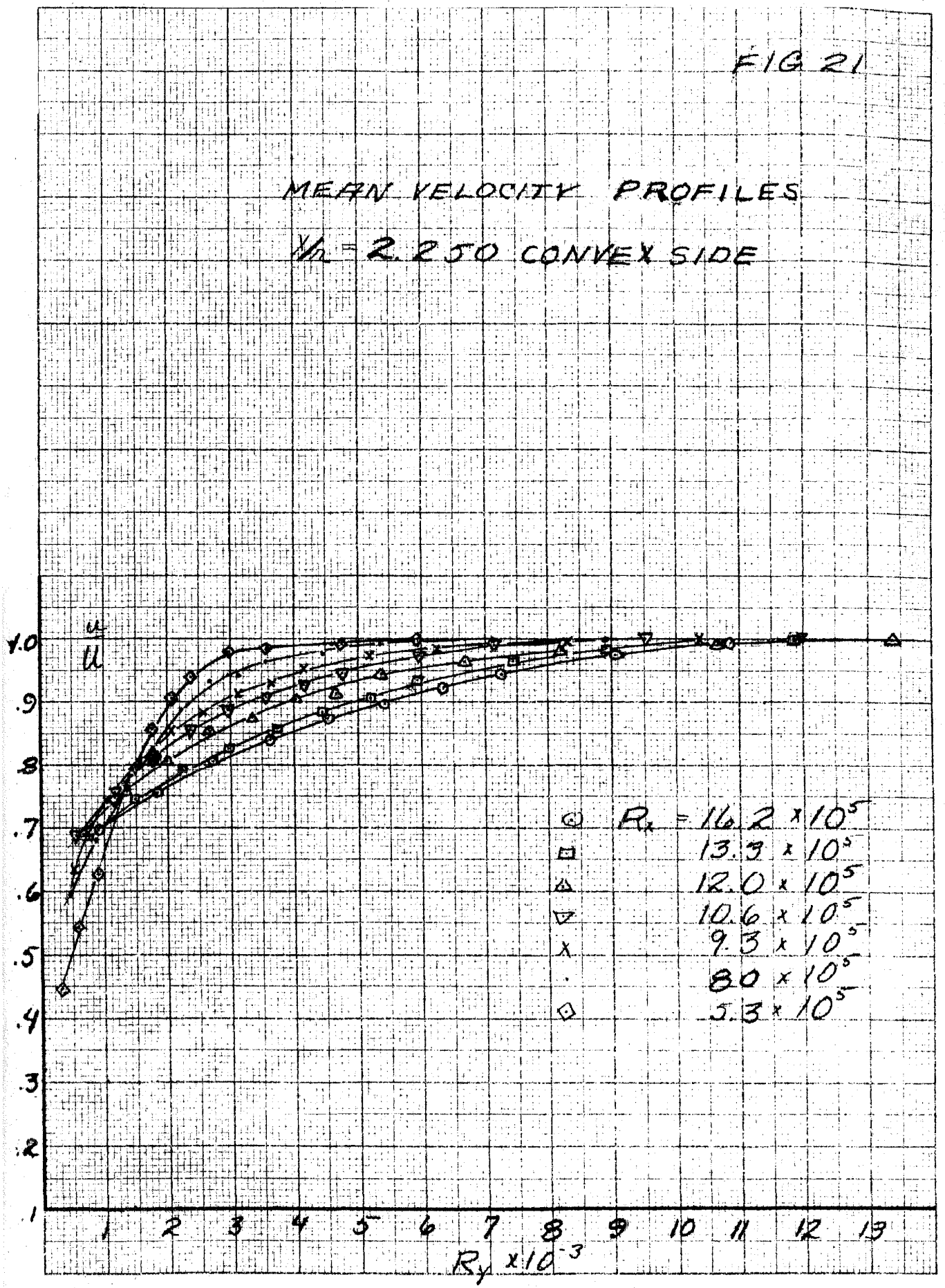

FIG. 22

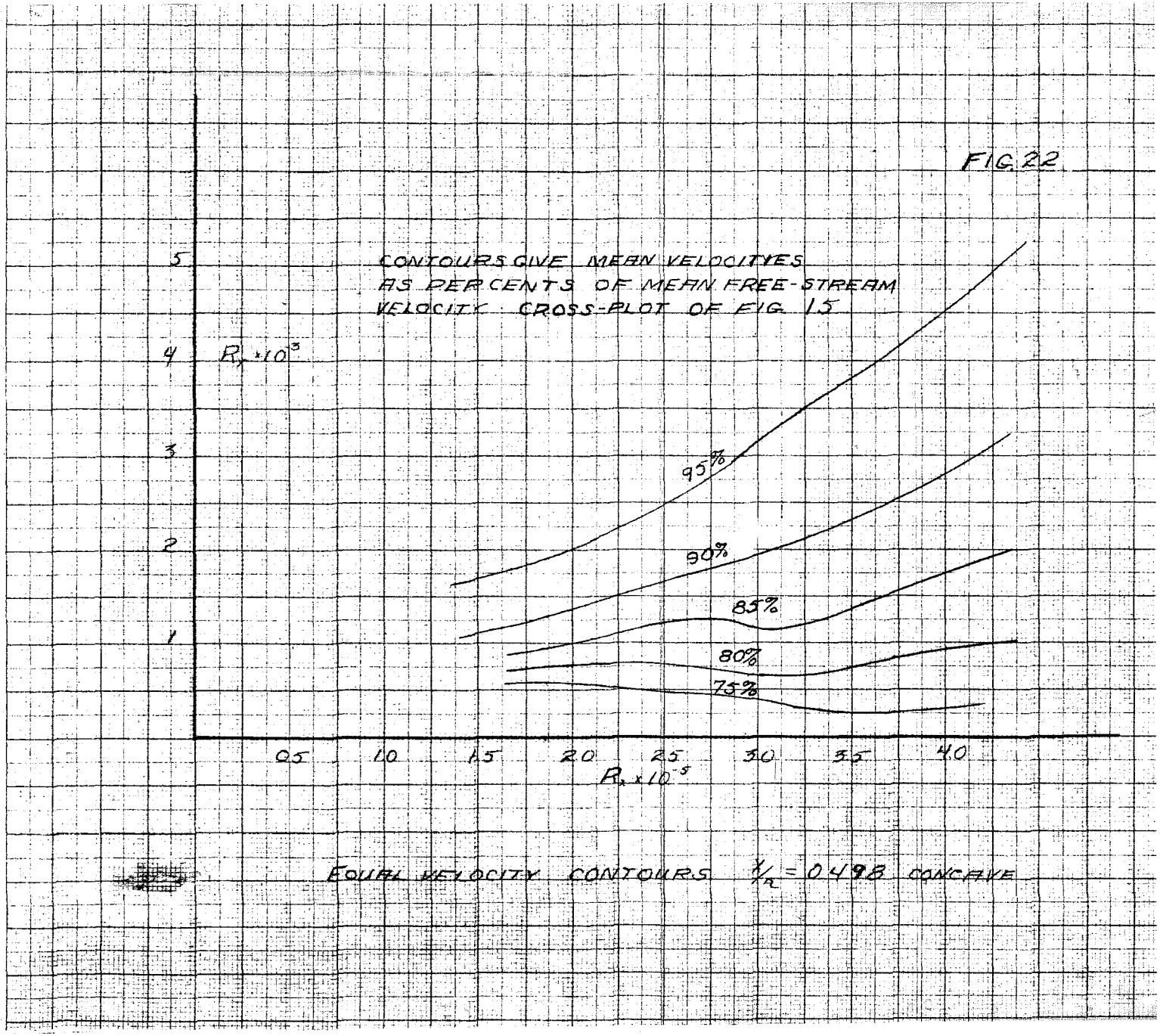


EQUAL VELOCITY CONTOURS $x/L = 0.498$ CONCAVE

FIG 23

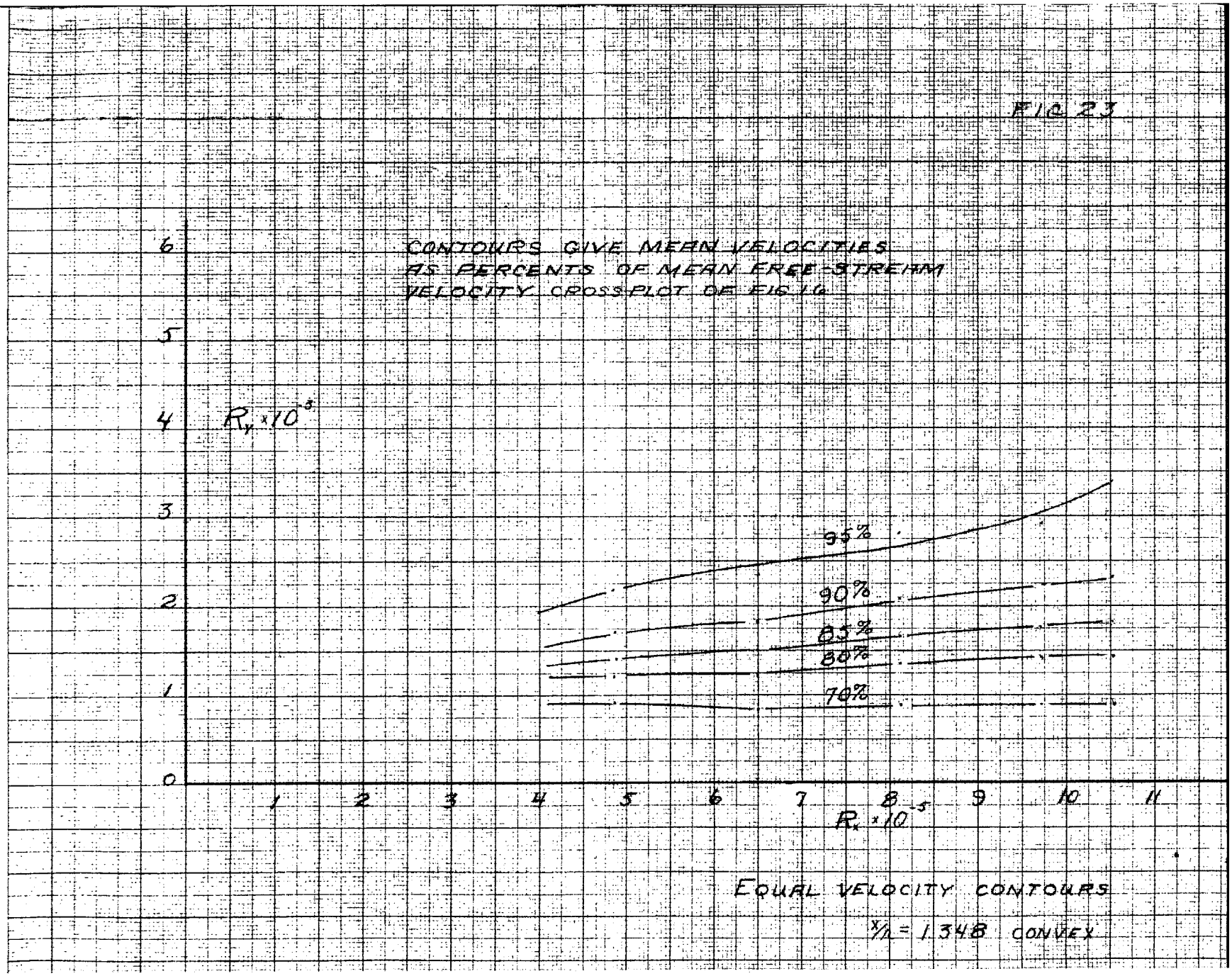


EQUAL VELOCITY CONTOURS

$x/L = 1.348$ CONVEX

FIG. 24.

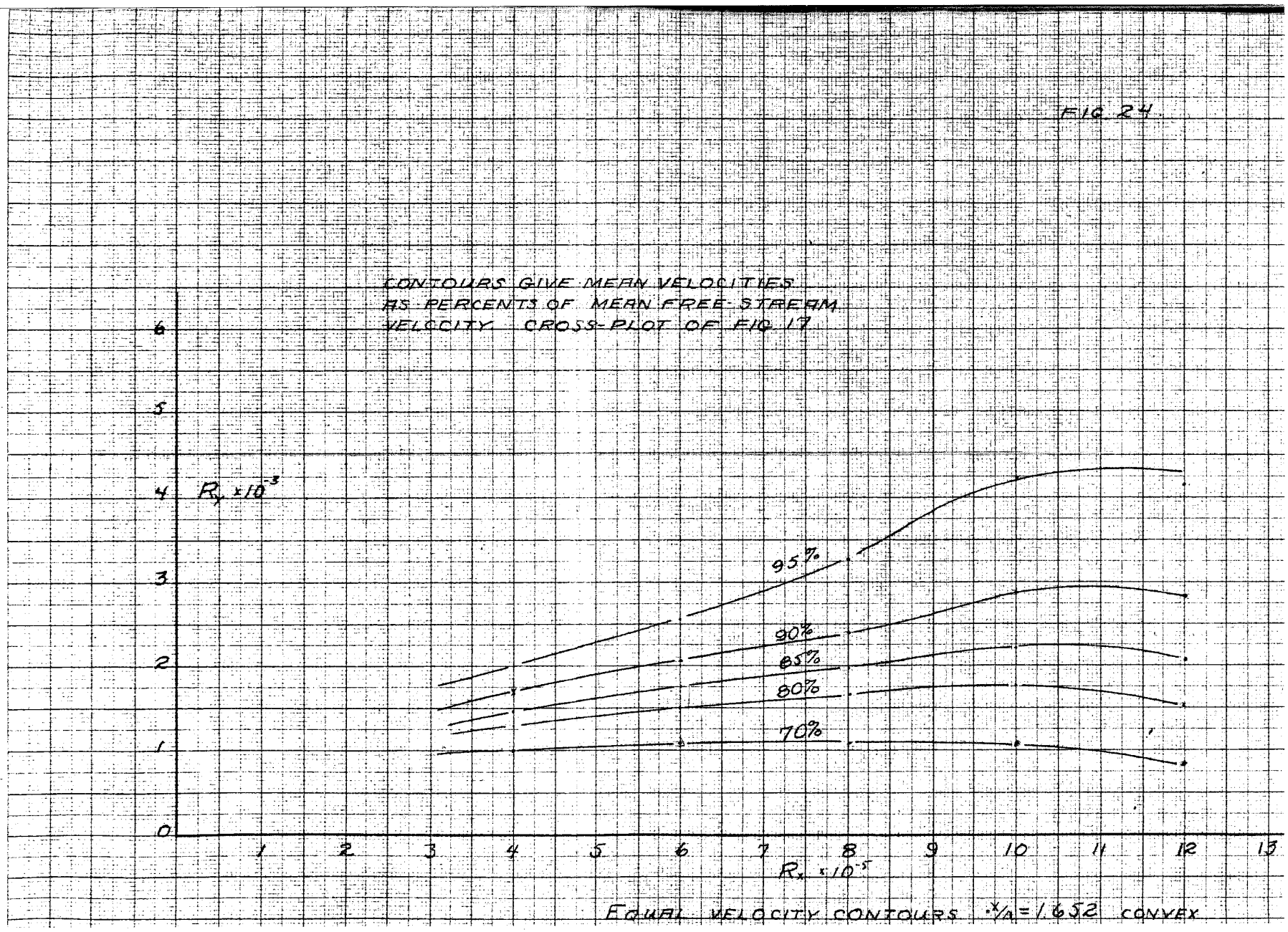


EQUAL VELOCITY CONTOURS $^{x}/_{A} = 1.652$ CONVEX

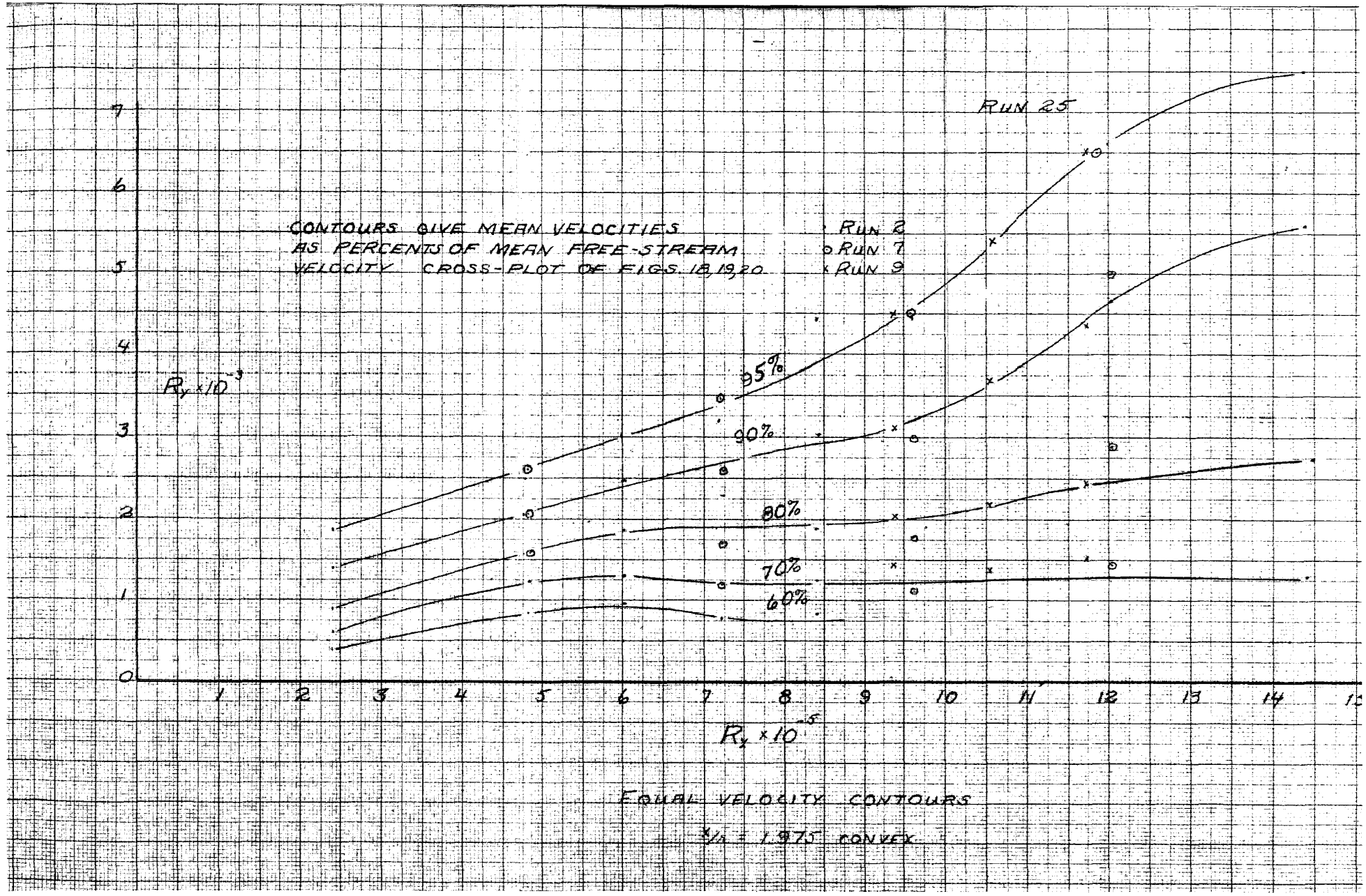


EQUAL VELOCITY CONTOURS

$x/L = 1.975$ CONVEX

FIG 26

CONTOURS GIVE MEAN VELOCITIES AS PERCENTS OF MEAN FREE-STREAM VELOCITY. CROSS-PLOT OF FIG 21

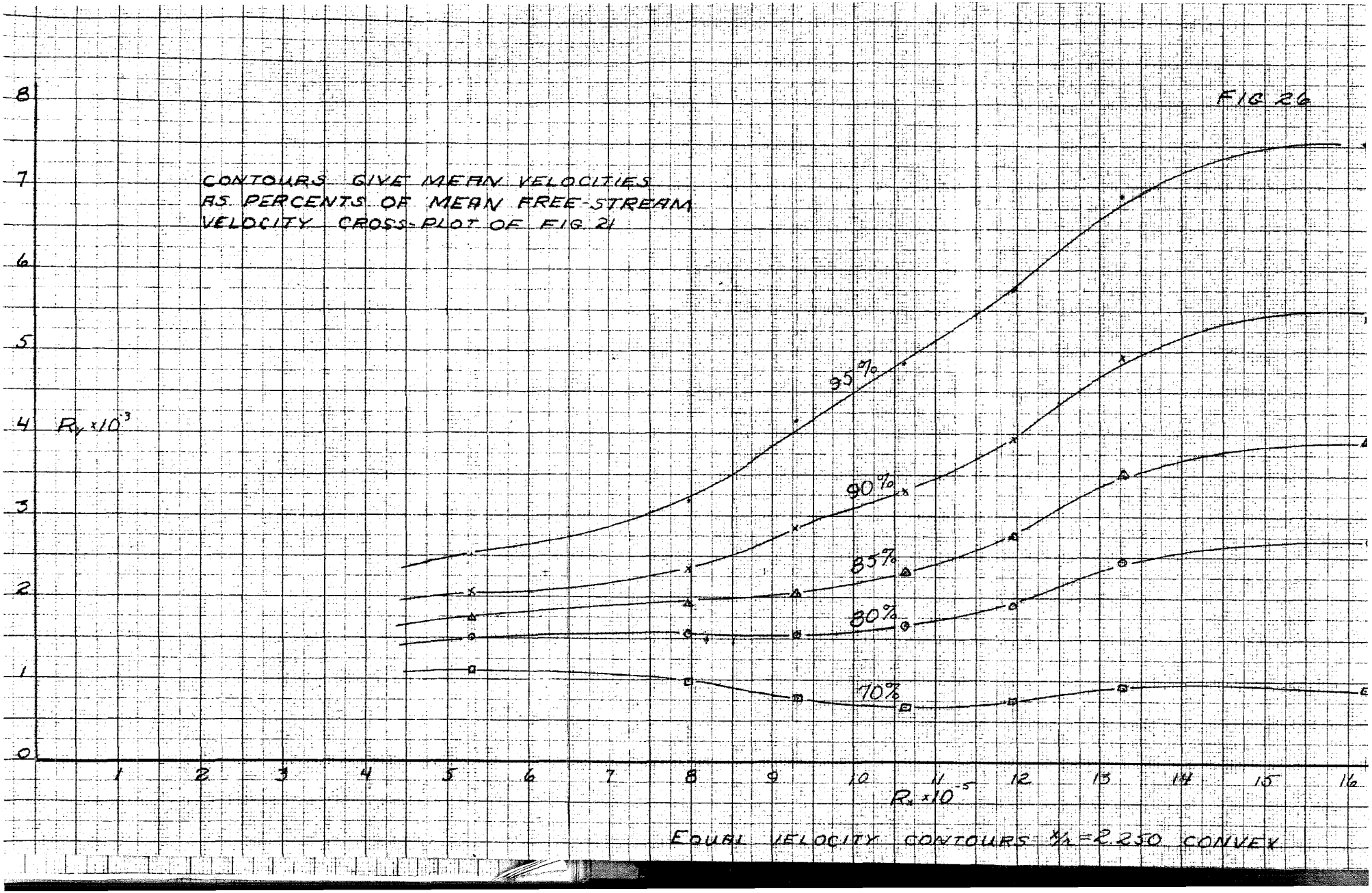


EQUAL VELOCITY CONTOURS $x/L = 2.250$ CONVEX

FIG 27

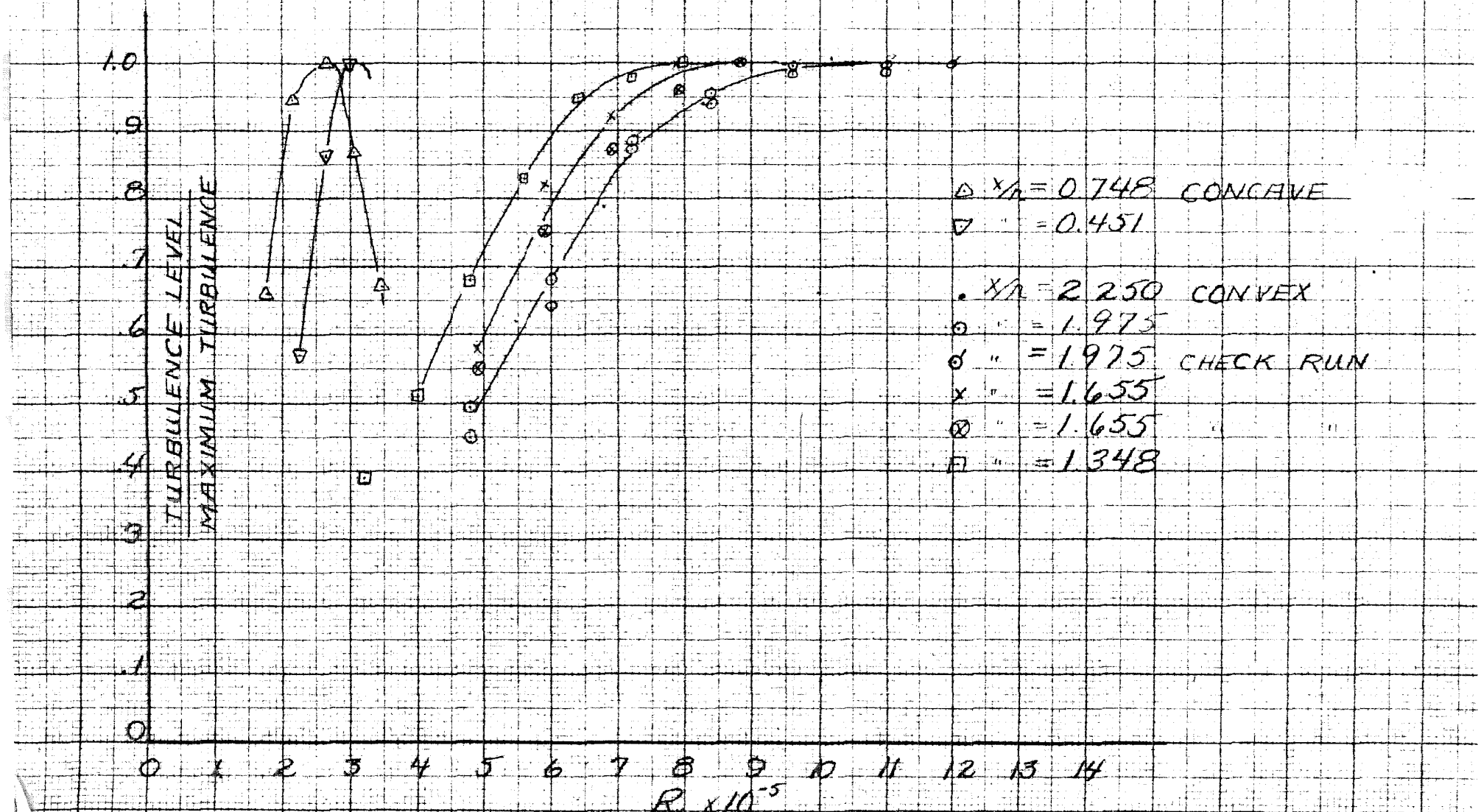


TURBULENCE READINGS AS FUNCTION OF $R_x$ FOR VARIOUS VALUES OF $x/L$

FIG. 28

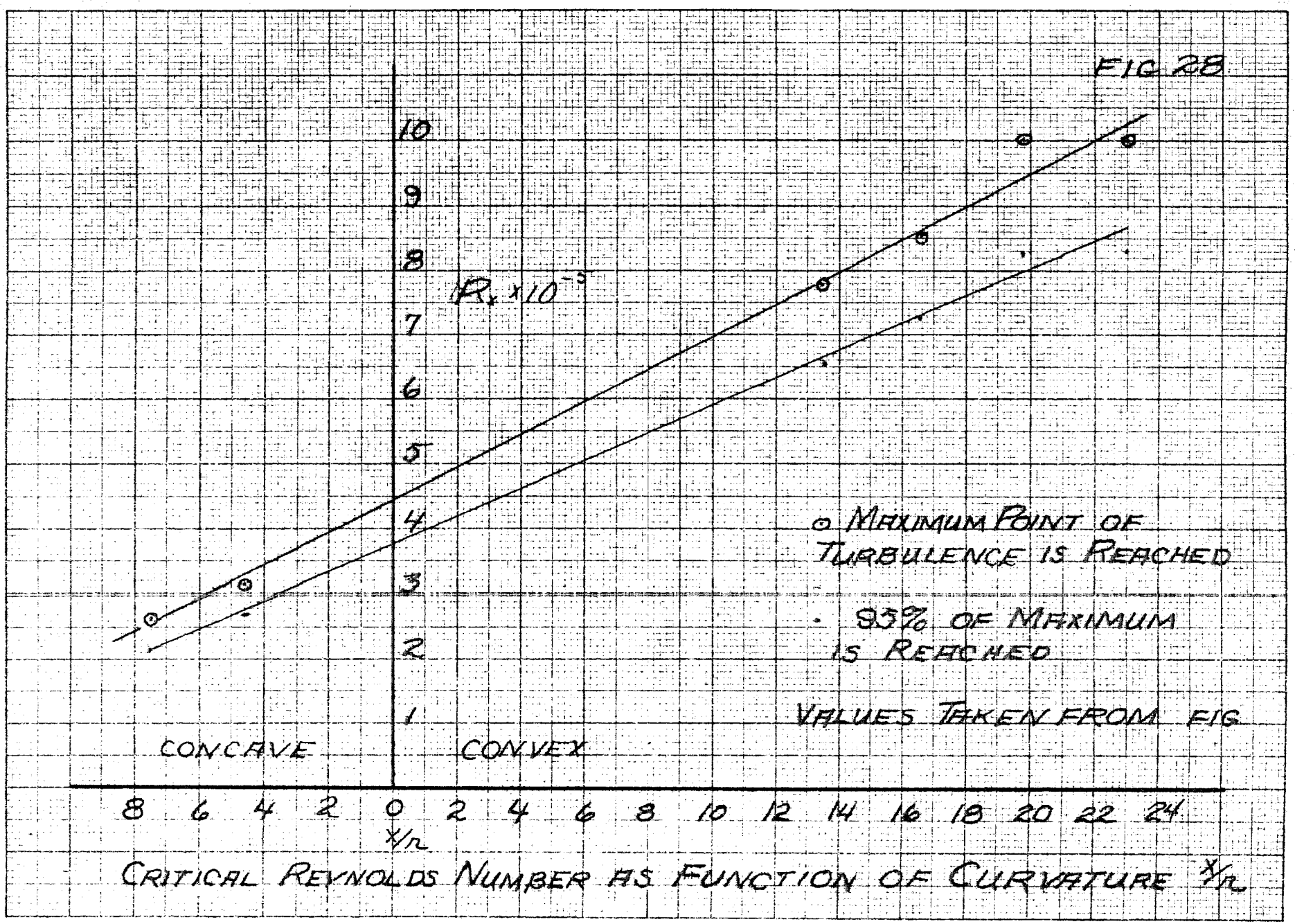


CRITICAL REYNOLDS NUMBER AS FUNCTION OF CURVATURE $x/r$

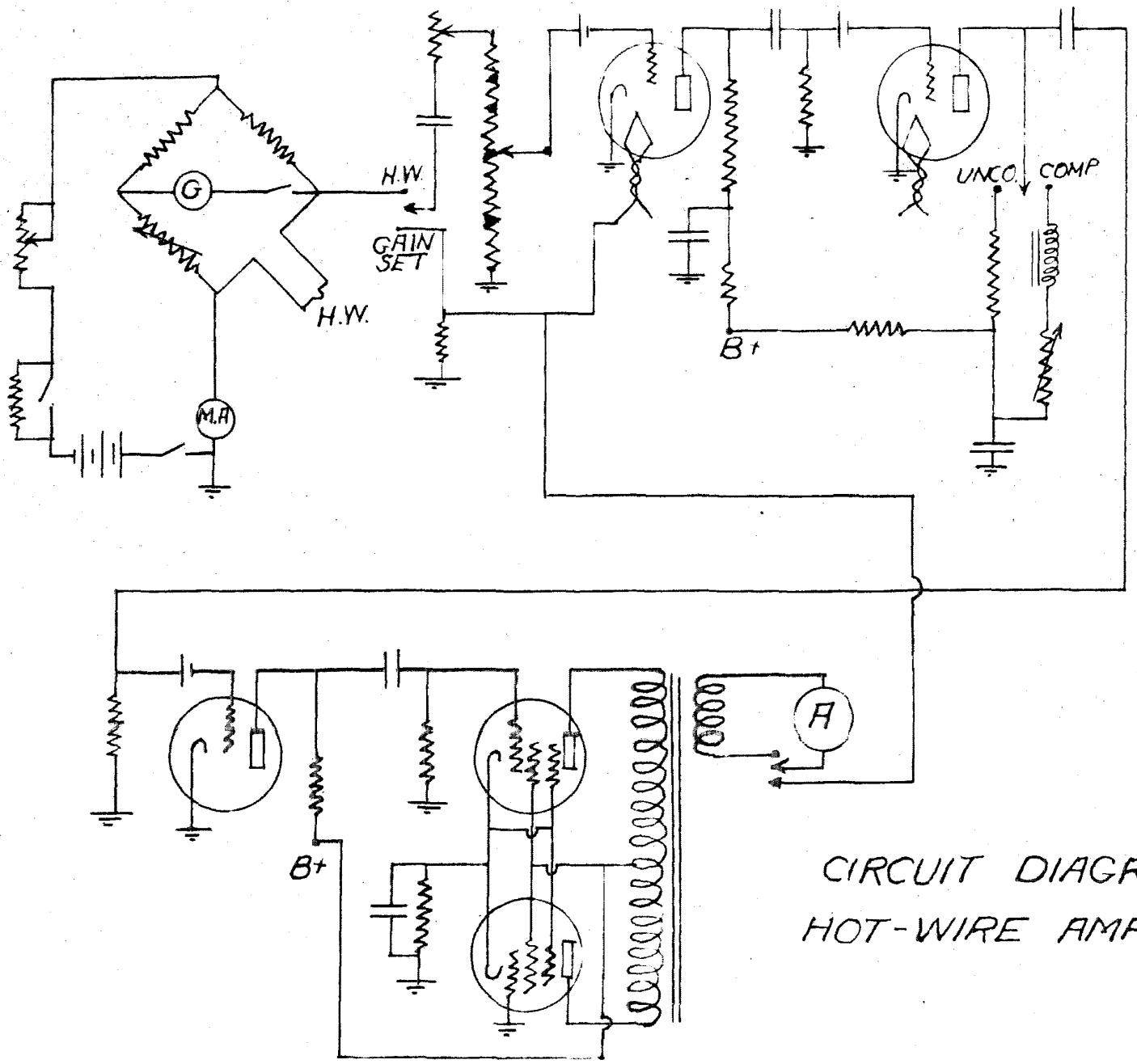


CIRCUIT DIAGRAM OF HOT-WIRE AMPLIFIER

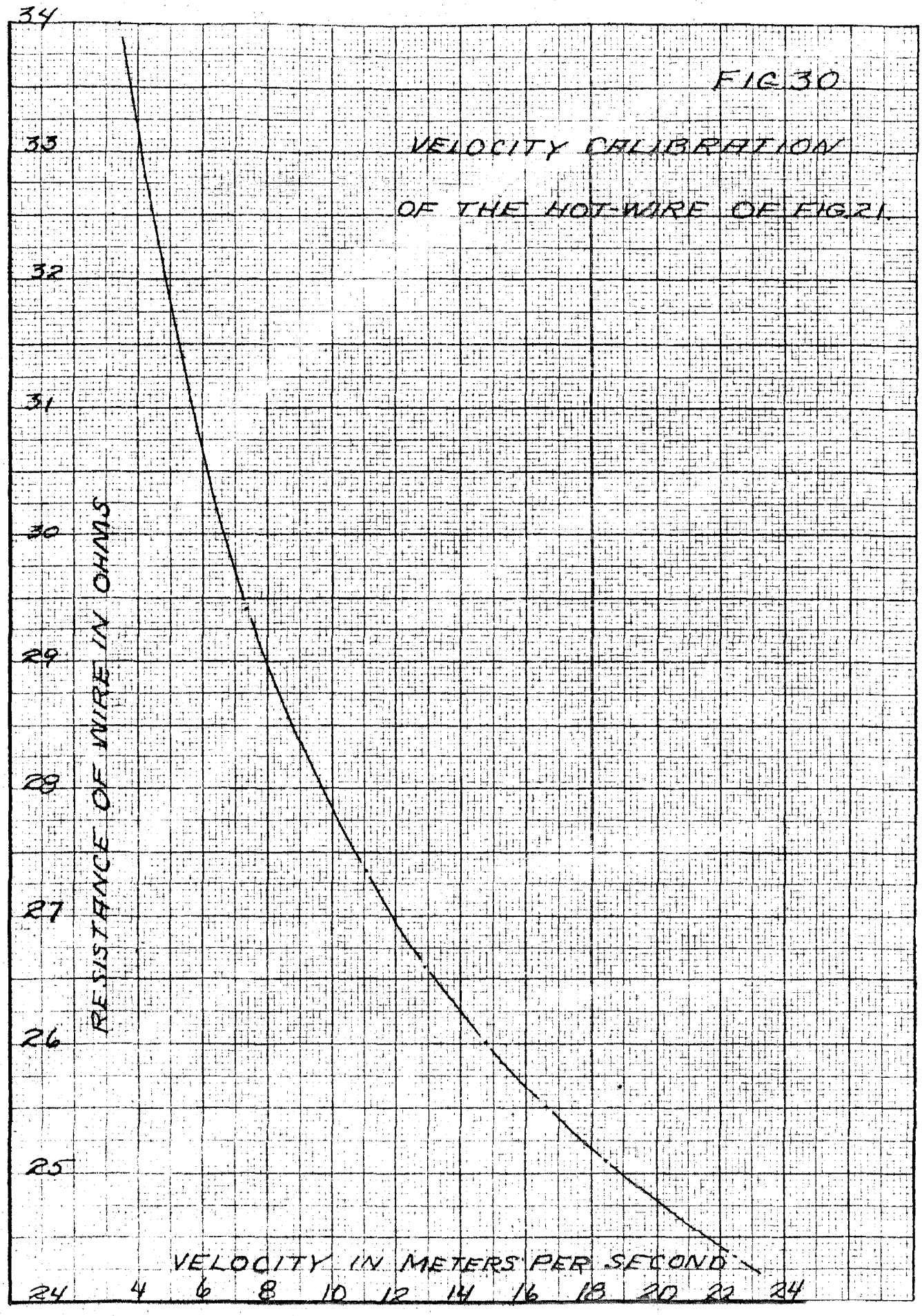
FIG 30
VELOCITY CALIBRATION
OF THE HOT-WIRE OF FIG. 21.
RESISTANCE OF WIRE IN OHMS
34
33
32
31
30
29
28
27
26
25
VELOCITY IN METERS PER SECOND
24
4
6
8
10
12
14
16
18
20
22
24

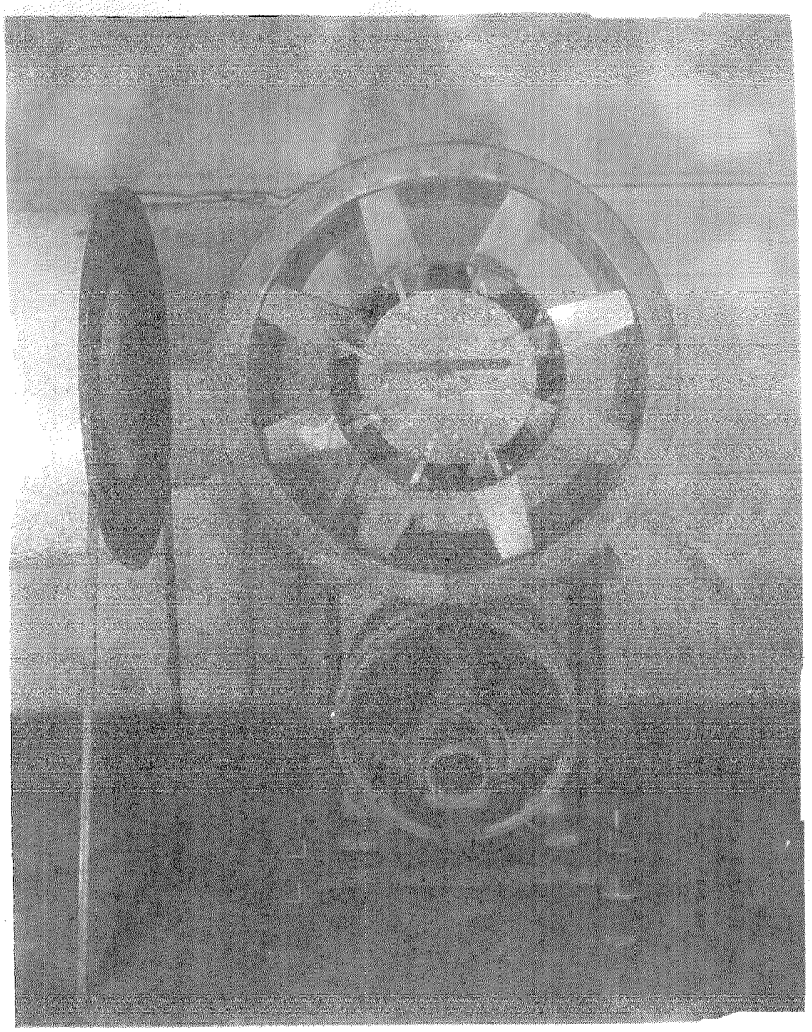

Photo 1

Fan Assembly Detached from Diffuser.

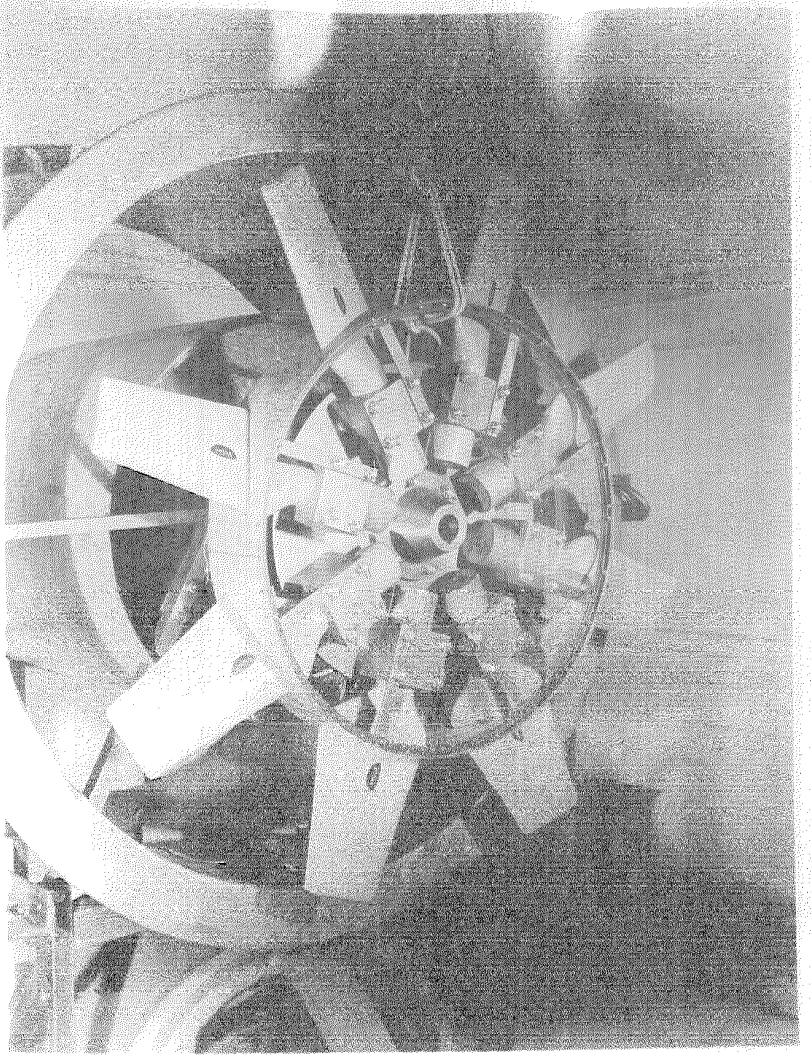

Photo 2

Fan about to be mounted.

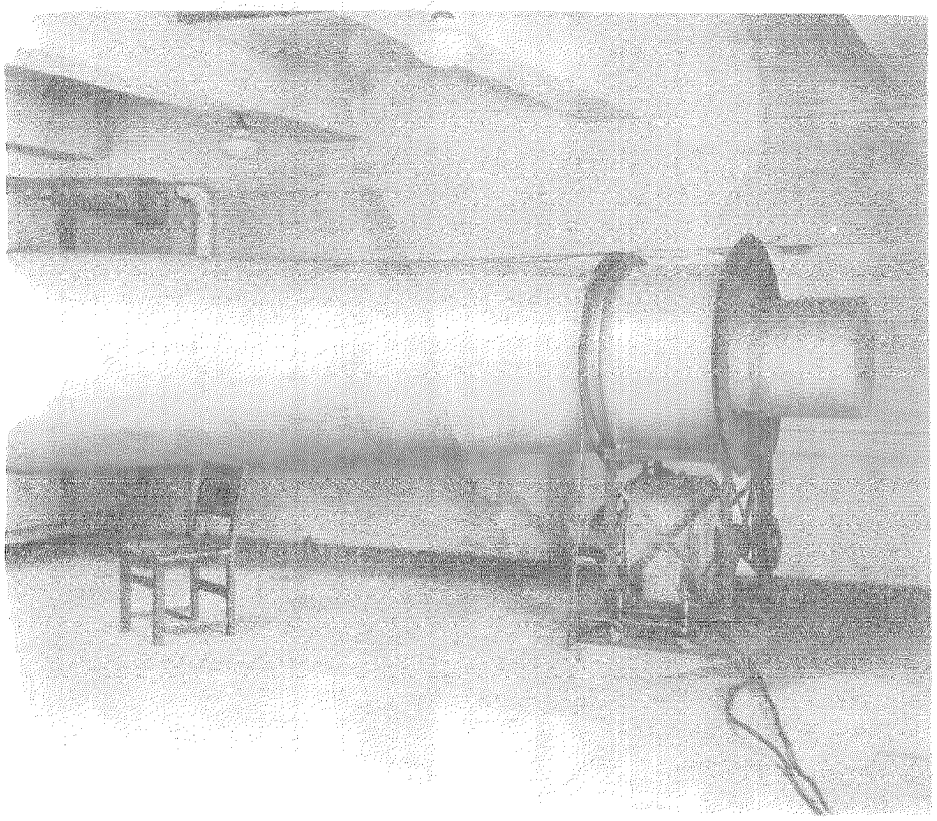

Photo 3

Fan Assembly and Diffuser.

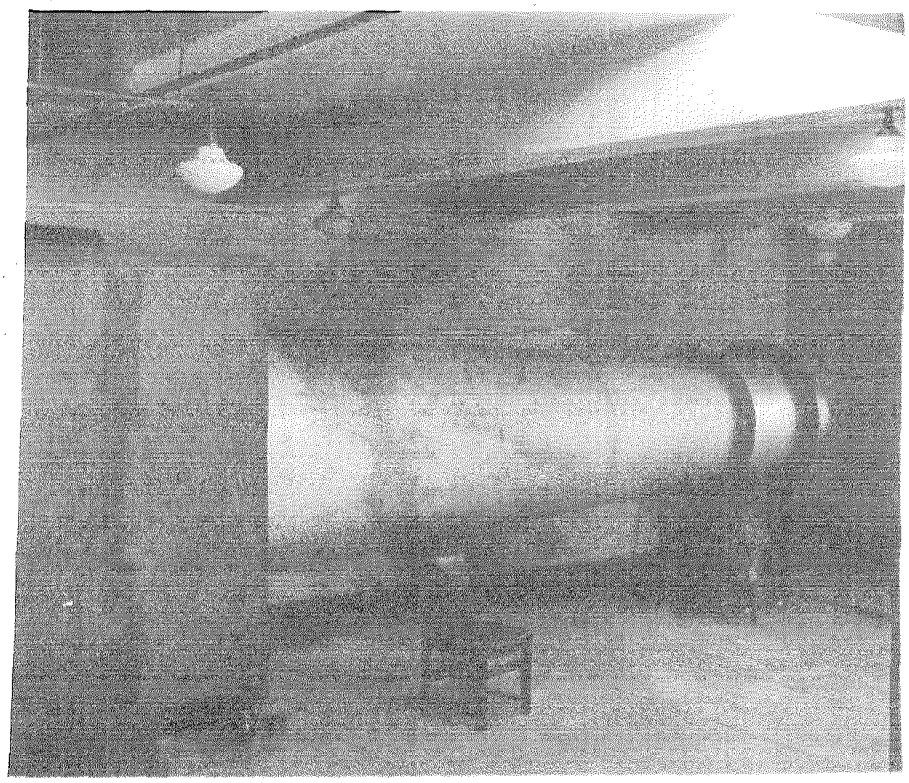

Photo 4

Diffuser Section.

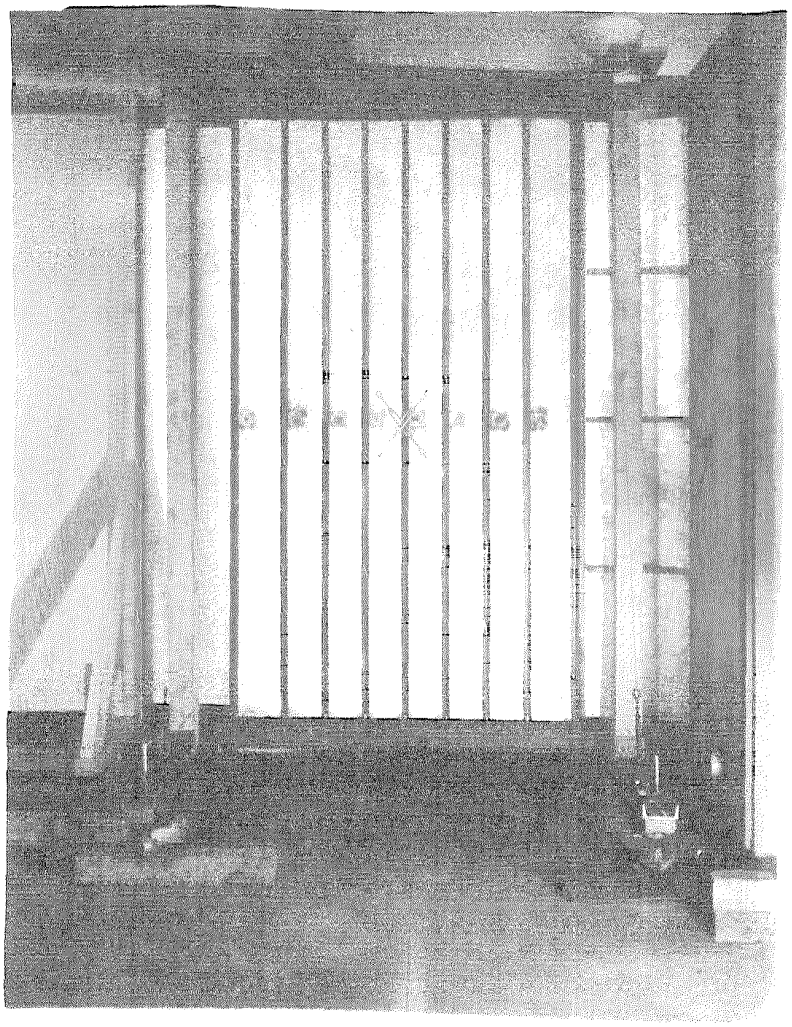

Photo 5

Straight Working Section.

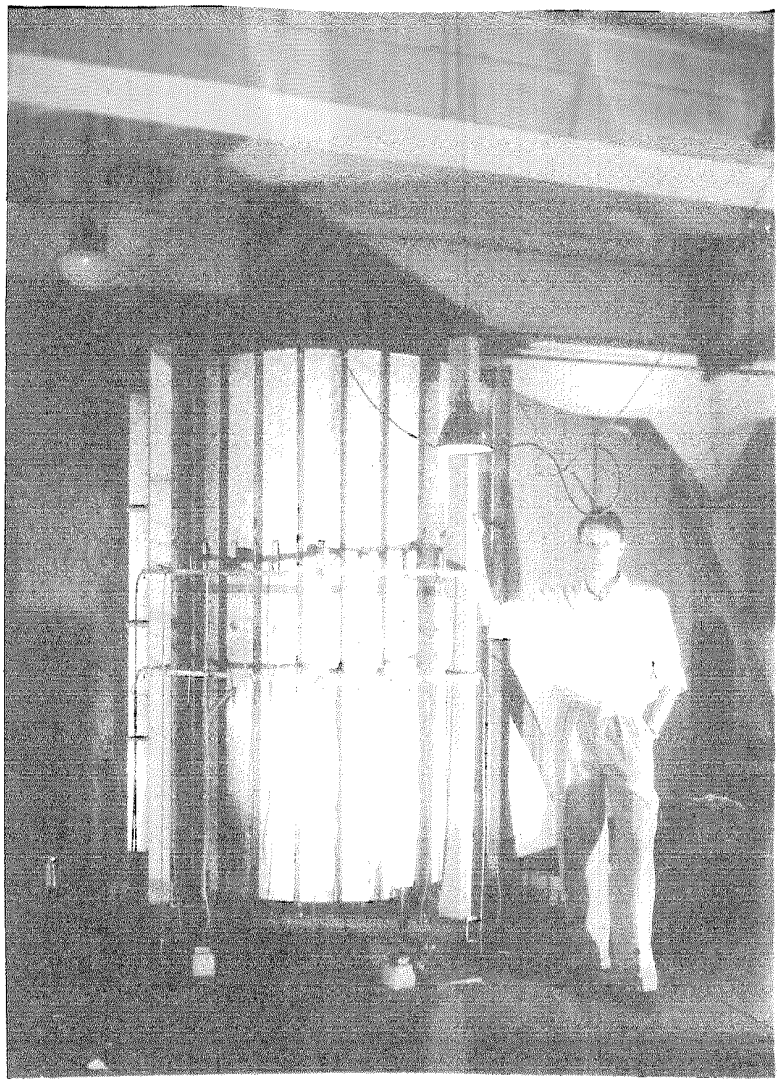

Photo 6

Curved Working Section.

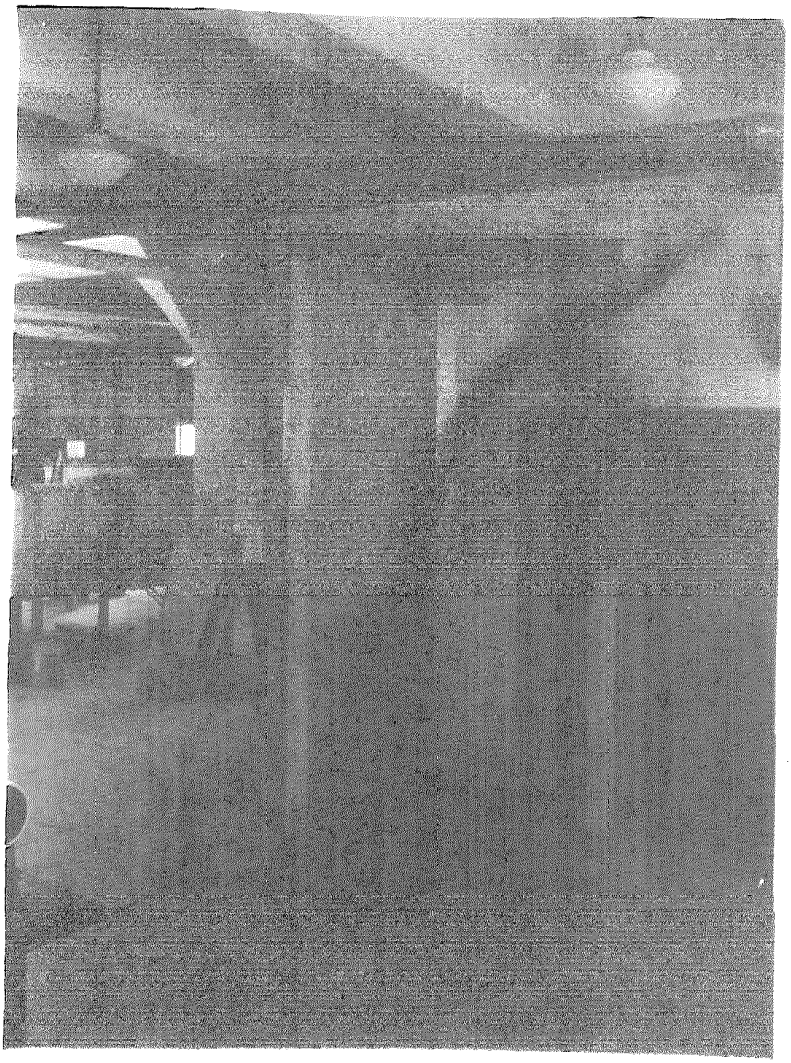

Photo 7

Framework of Curved Working Section.

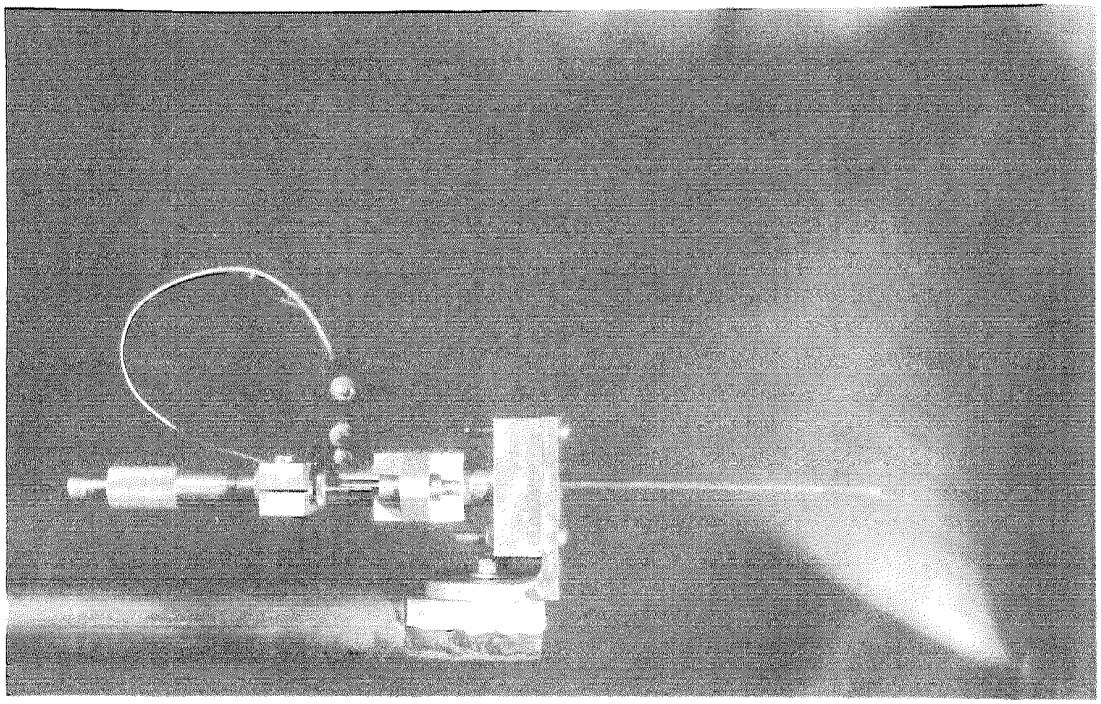

Photo 8

Micrometer Carriage Hot-Wire Holder.

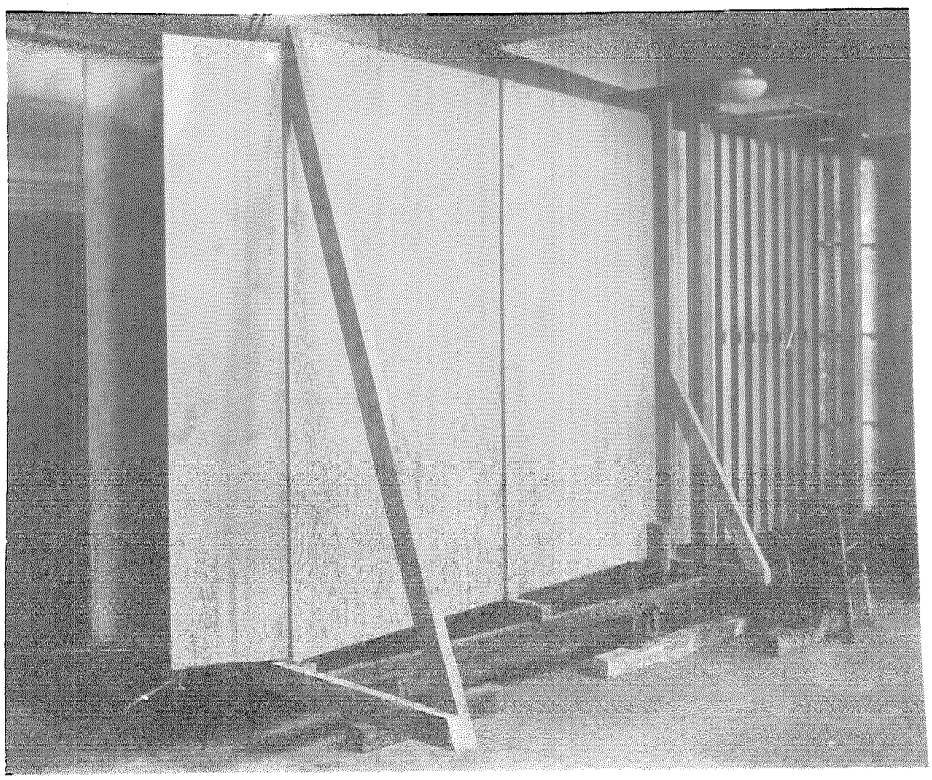

Photo 9

Exit Diffuser.

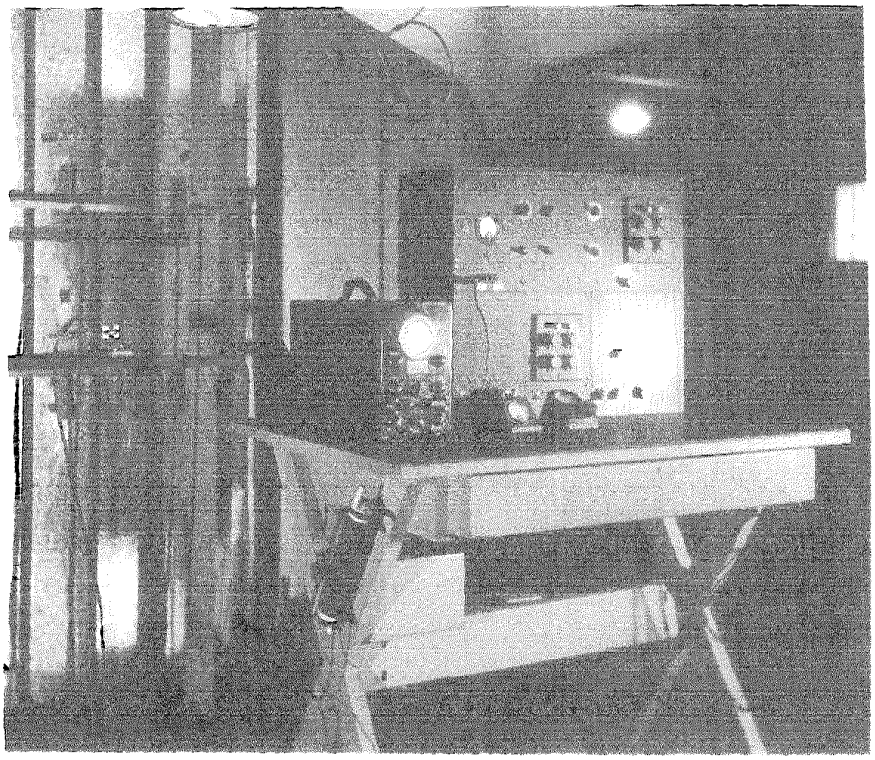

Photo 10

Hot-Wire Amplifier.

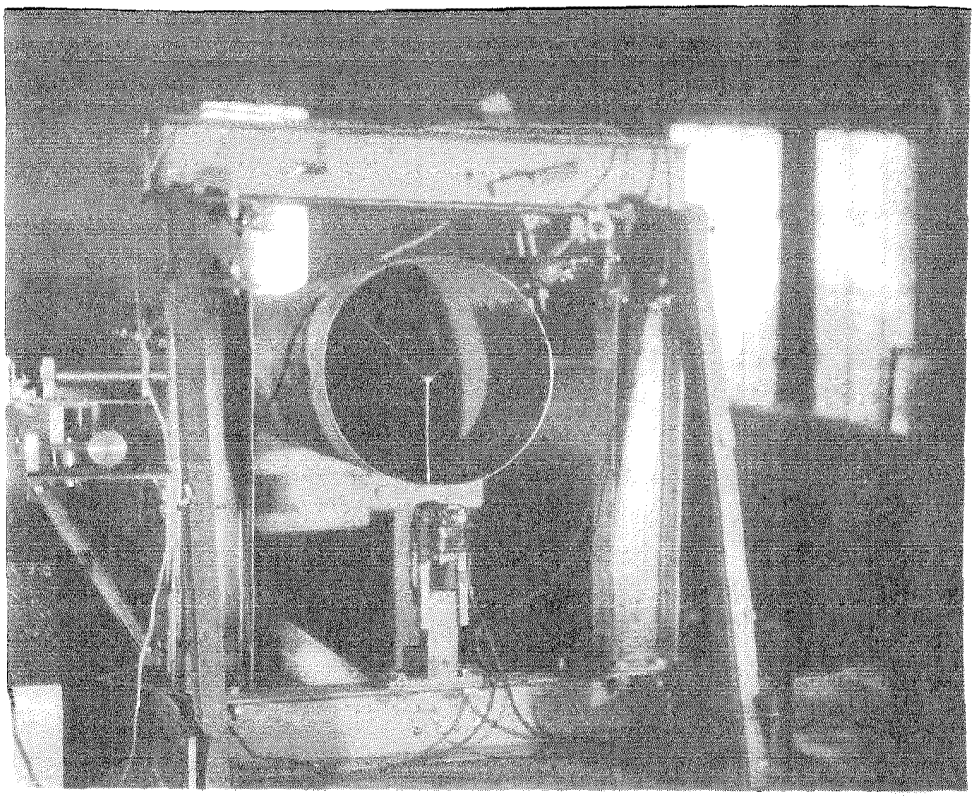

Photo 11

Calibrating Tunnel.